Article

Multi-Ancestry Transcriptome-Wide Association Studies of Cognitive Function, White Matter Hyperintensity, and Alzheimer's Disease

Dima L. Chaar [1] , Zheng Li [2] , Lulu Shang [3], Scott M. Ratliff [1], Thomas H. Mosley [4] , Sharon L. R. Kardia [1], Wei Zhao [1,5] , Xiang Zhou [2] and Jennifer A. Smith [1,5,*]

[1] Department of Epidemiology, School of Public Health, University of Michigan, Ann Arbor, MI 48109, USA; dimachaar1@gmail.com (D.L.C.); ratliffs@umich.edu (S.M.R.); skardia@umich.edu (S.L.R.K.); zhaowei@umich.edu (W.Z.)

[2] Department of Biostatistics, School of Public Health, University of Michigan, Ann Arbor, MI 48109, USA; zlisph@umich.edu (Z.L.); xzhousph@umich.edu (X.Z.)

[3] Department of Biostatistics, University of Texas MD Anderson Cancer Center, Houston, TX 77030, USA; shanglu@umich.edu

[4] Memory Impairment and Neurodegenerative Dementia (MIND) Center, University of Mississippi Medical Center, Jackson, MS 39216, USA; tmosley@umc.edu

[5] Survey Research Center, Institute for Social Research, University of Michigan, Ann Arbor, MI 48104, USA

* Correspondence: smjenn@umich.edu

Abstract: Genetic variants increase the risk of neurocognitive disorders in later life, including vascular dementia (VaD) and Alzheimer's disease (AD), but the precise relationships between genetic risk factors and underlying disease etiologies are not well understood. Transcriptome-wide association studies (TWASs) can be leveraged to better characterize the genes and biological pathways underlying genetic influences on disease. To date, almost all existing TWASs on VaD and AD have been conducted using expression studies from individuals of a single genetic ancestry, primarily European. Using the joint likelihood-based inference framework in Multi-ancEstry TRanscriptOme-wide analysis (METRO), we leveraged gene expression data from European ancestry (EA) and African ancestry (AA) samples to identify genes associated with general cognitive function, white matter hyperintensity (WMH), and AD. Regions were fine-mapped using Fine-mapping Of CaUsal gene Sets (FOCUS). We identified 266, 23, 69, and 2 genes associated with general cognitive function, WMH, AD (using EA GWAS summary statistics), and AD (using AA GWAS), respectively (Bonferroni-corrected alpha = $p < 2.9 \times 10^{-6}$), some of which had been previously identified. Enrichment analysis showed that many of the identified genes were in pathways related to innate immunity, vascular dysfunction, and neuroinflammation. Further, the downregulation of *ICA1L* was associated with a higher WMH and with AD, indicating its potential contribution to overlapping AD and VaD neuropathology. To our knowledge, our study is the first TWAS on cognitive function and neurocognitive disorders that used expression mapping studies for multiple ancestries. This work may expand the benefits of TWASs beyond a single ancestry group and help to identify gene targets for pharmaceuticals or preventative treatments for dementia.

Keywords: cognitive function; Alzheimer's disease; white matter hyperintensity; dementia; vascular dementia; transcriptome-wide association study; multi-ancestry

1. Introduction

Adult-onset dementia comprises a group of aging-related neurocognitive disorders caused by the gradual degeneration of neurons and the loss of brain function. These changes lead to a decline in cognitive abilities and impairments in daily activities and independent function. In the United States, Alzheimer's disease (AD), the most common cause of dementia, affects 6.8 million adults aged 65 and older [1]. The second most common form of dementia is vascular dementia (VaD), which often co-occurs with AD and is underdiagnosed [1,2]. VaD is often difficult to distinguish from AD because these diseases share cognitive symptoms, including noticeable impairments in episodic and semantic memory. While AD and VaD often co-occur, each form of dementia has a differing pathophysiology that may precede the illness decades prior.

AD is characterized by the aggregation of amyloid-beta protein and neurofibrillary tangles in brain tissue [3,4], while VaD may be caused by reduced blood flow to the brain as a result of small vessel disease (SVD) or stroke and is commonly seen in people with hypertension [5]. AD is diagnosed based on a battery of memory tests, brain imaging tests to evaluate the degeneration of brain cells, and laboratory tests to assess the presence of amyloid and tau proteins in cerebrospinal fluid [6]. SVD is primarily detected on magnetic resonance imaging (MRI) as white matter hyperintensities (WMHs). It has been hypothesized that vascular and neurodegenerative changes in the brain may interact in ways that increase the likelihood of cognitive impairment. A further challenge in the field is distinguishing between individuals who are aging normally from those with dementia pathology.

A greater understanding of the pathological processes that influence cognitive function in older adults is critical for early intervention during the long preclinical or prodromal phase prior to dementia onset, especially in vulnerable populations [7,8]. For example, African American individuals have a greater burden of and risk for developing dementia compared to non-Hispanic white individuals [9–12]. Differences in gene expression, which are influenced by both genetic and non-genetic factors, may play a role in shaping racial health disparities in neurological outcomes. However, the underlying molecular and environmental mechanisms that influence gene expression are not fully understood, especially in ancestrally diverse populations. Given the multifactorial and complex nature of dementia, multi-omic data integration across ancestry groups may lend insight into these disparities, allowing for the identification of targets for intervention and treatment in populations that are most at risk [13].

Genome-wide association studies (GWASs) have identified genetic variants associated with cognitive function and dementia; however, most GWAS variants are located in non-coding regions, so their functional consequences are difficult to characterize [14]. Transcriptome-wide association studies (TWASs) utilize gene expression and genetic data to increase the power for identifying gene–trait associations and characterizing the gene expression mechanisms underlying complex diseases. To date, however, few TWASs have been conducted on cognitive or structural brain measures. Further, previous TWASs have primarily been conducted in populations of European ancestry (EA), but these results cannot always be generalized to other genetic ancestries due to differences in allele frequencies, patterns of linkage disequilibrium (LD), and the relationships between single-nucleotide polymorphisms (SNPs) and gene expression among populations [15–18]. To better identify gene–trait associations in non-European ancestries, it is necessary to incorporate results from recent expression quantitative trait locus (eQTL) mapping studies, which identify genetic variants that explain variations in gene expression levels, conducted in different ancestry groups [19].

Multi-ancEstry TRanscriptOme-wide analysis (METRO) [20] is a TWAS method that uses a joint likelihood-based inference framework to borrow complementary information across multiple ancestries to increase TWAS power. In this study, we employed a multi-ancestry TWAS with the Genetic Epidemiology Network of Arteriopathy (GENOA) dataset (1032 African ancestry (AA) and 801 EA individuals) to identify genes associated with general cognitive function [21], white matter hyperintensity [22], and AD [23,24]. We then examined the contributions of different ancestry-dependent gene expression profiles to the gene–trait associations. Obtaining greater knowledge of the underlying molecular mechanisms of dementia that are generalizable to both EA and AA individuals is a critical step in evaluating potential causal variants and genes that could be targeted for pharmaceutical development.

2. Results

In Table 1, we provide descriptive statistics for the samples used in the eQTL mapping study (e.g., 1032 AA and 801 EA individuals from GENOA) and the four input GWASs [21–23]. The GENOA eQTL study included participants with a mean age of 56.9 (SD = 10.0) years. More than half of the participants were female (65.6%). The mean age of the participants was 56.9 (SD = 7.8) years in the general cognitive function GWAS [21], and 64.2 years in the WMH GWAS [22]. In the AD GWAS in the EA population [23], the mean age was 73.6 (SD = 8.1) years for cases and 67.9 (SD = 8.6) years for controls. In the AD GWAS in the AA population [24], the mean age was 74.2 (SD = 13.6) years for all participants.

Table 1. Sample characteristics of expression quantitative trait locus (eQTL) mapping study and genome-wide association study (GWAS) participants.

eQTL mapping study: Genetic Epidemiology Network of Arteriopathy (GENOA)		
		Mean (SD) or N (%) or N
N		1833
Age (years)		56.85 (10.0)
Female		1202 (65.6%)
Race/Ethnicity		
	African Americans	1032 (56.3%)
	European Americans	801 (43.7%)
General cognitive function GWAS: CHARGE, COGENT, UKB [a]		
		Mean (SD) or N (%) or N
N		300,486
Age (years)		56.91 (7.8)
Female		156,854 (52.2%)
Excluded for dementia and/or stroke diagnosis (N)		4919
White matter hyperintensity (WMH) GWAS: CHARGE and UKB [a]		
		Mean (SD) or N (%) or N
N		48,454
Age (years)		64.17
Female		29,215 (57.6%)
WMH volume (cm^3)		7.06 (8.8)
Excluded for stroke or pathologies (N)		1572

Table 1. *Cont.*

EA Alzheimer's Disease (AD) GWAS: EADB, GR@ACE, EADI, GERAD/PERADES, DemGene, Bonn, the Rotterdam study, the CCHS study, NxC, and the UKB [a]		
		Mean (SD) or N (%) or N
Discovery sample		
	AD cases (N)	39,106
	AD proxy cases (N)	46,828
	Controls (N)	401,577
Age (years)		
	AD cases or proxy cases	73.55 (8.1)
	Controls	67.86 (8.6)
Female		
	AD cases or proxy cases (N)	54,052 (62.9%)
	Controls (N)	48,209 (56.1%)
AA Alzheimer's Disease (AD) GWAS: AD Genetics Consortium [b]		
		Mean (SD) or N (%) or N
N		7970
	AD cases	2748 (34.5%)
	Controls	5222 (65.5%)
Age (years)		74.2 (13.6)
Female		
	AD cases	1944 (69.8%)
	Controls	3743 (71.7%)

Abbreviations: EA, European ancestry; AA, African ancestry. [a] GWASs [21–23] include only European ancestry participants. [b] GWAS [24] includes only African ancestry participants.

Using METRO, we identified 602 genes associated with general cognitive function, 45 genes associated with WMH, 231 genes associated with AD (EA GWAS), and 9 genes associated with AD (AA GWAS) that were significant at the Bonferroni-corrected alpha level ($p < 2.90 \times 10^{-6}$; Figure 1, Tables S1–S3).

The genomic inflation factors for the TWAS p-values ranged from 1.00 to 2.55 (Figure 2). Among the three neurocognitive outcomes, prior to fine-mapping, the METRO TWAS identified the *ICA1L* gene overlapping between WMH ($\alpha = -0.27$; $p = 5.44 \times 10^{-12}$) and AD (from EA GWAS; $\alpha = -0.06$; $p = 2.68 \times 10^{-6}$); the *FMNL1* gene overlapping between WMH ($\alpha = 0.54$; $p = 1.39 \times 10^{-8}$) and general cognitive function ($\alpha = 0.17$; $p = 2.15 \times 10^{-6}$); and 22 genes enriched in AD-related pathways and functions overlapping between general cognitive function and AD (from EA GWAS) (Figures 3a and S1). After fine-mapping, the only overlapping gene that remained was *ICA1L* between WMH and AD (Figure 3b). The METRO TWAS for AD (AA GWAS) identified nine genes overlapping with those identified in AD (EA GWAS); however, following fine-mapping, only *TOMM40* overlapped between the two AD TWASs (EA TWAS: $\alpha = -19.78$; $p = 4.77 \times 10^{-39}$; AA TWAS: $\alpha = 10.02$; $p = 1.15 \times 10^{-80}$; Figure 3b).

For all identified genes, we also examined the contribution weights of expression prediction models for the EA and AA ancestries, prior to fine-mapping ($p < 2.90 \times 10^{-6}$; Figure 4). For the WMH TWAS, a significantly higher proportion of genes had a greater contribution from EA weights than AA weights (65.2% vs. 34.8%). This is consistent with Li et al. (2022) [20], who found that gene expression prediction models constructed in the same ancestry as the input GWAS, in this case EA, often had larger contribution weights than those constructed in other ancestries. However, for both general cognitive function and AD (EA and AA GWASs), the contributions from EA and AA weights were similar, which likely increased the power to identify genes relevant to AA.

After fine-mapping, there were 266 genes in the 90%-credible set across 172 different genomic regions for general cognitive function. This gene set included 82 genes that were not previously identified in the SNP-based GWAS results (mapped to the nearest gene) or the gene-based analysis results from Davies et al. (2018) [21] (Figure 5, Table S1); however, it is likely that some of these genes were in broader genomic regions tagged by the GWAS-identified SNPs. Specifically, there were 126 and 168 overlapping genes between METRO and the SNP-based and gene-based associations from Davies et al. (2018) [21], respectively (Figure 5). The 266 METRO-identified genes were enriched in regulatory pathways involved in protein binding ($p_{adj} = 1.17 \times 10^{-5}$), developmental cell growth ($p_{adj} = 3.33 \times 10^{-5}$), and the protein metabolic process ($p_{adj} = 7.18 \times 10^{-4}$), as well as neurodevelopmental processes such as neuron to neuron synapses ($p_{adj} = 1.22 \times 10^{-3}$) and neuron projection ($p_{adj} = 7.14 \times 10^{-3}$; Figure 6). The 82 genes that were not previously identified in Davies et al. (2018) [21] were enriched for the positive regulation of biological processes ($p_{adj} = 1.77 \times 10^{-2}$), the proteasome activator complex ($p_{adj} = 1.00 \times 10^{-2}$), nucleoplasm ($p_{adj} = 1.29 \times 10^{-2}$), and chromatin ($p_{adj} = 4.71 \times 10^{-5}$; Figure S2).

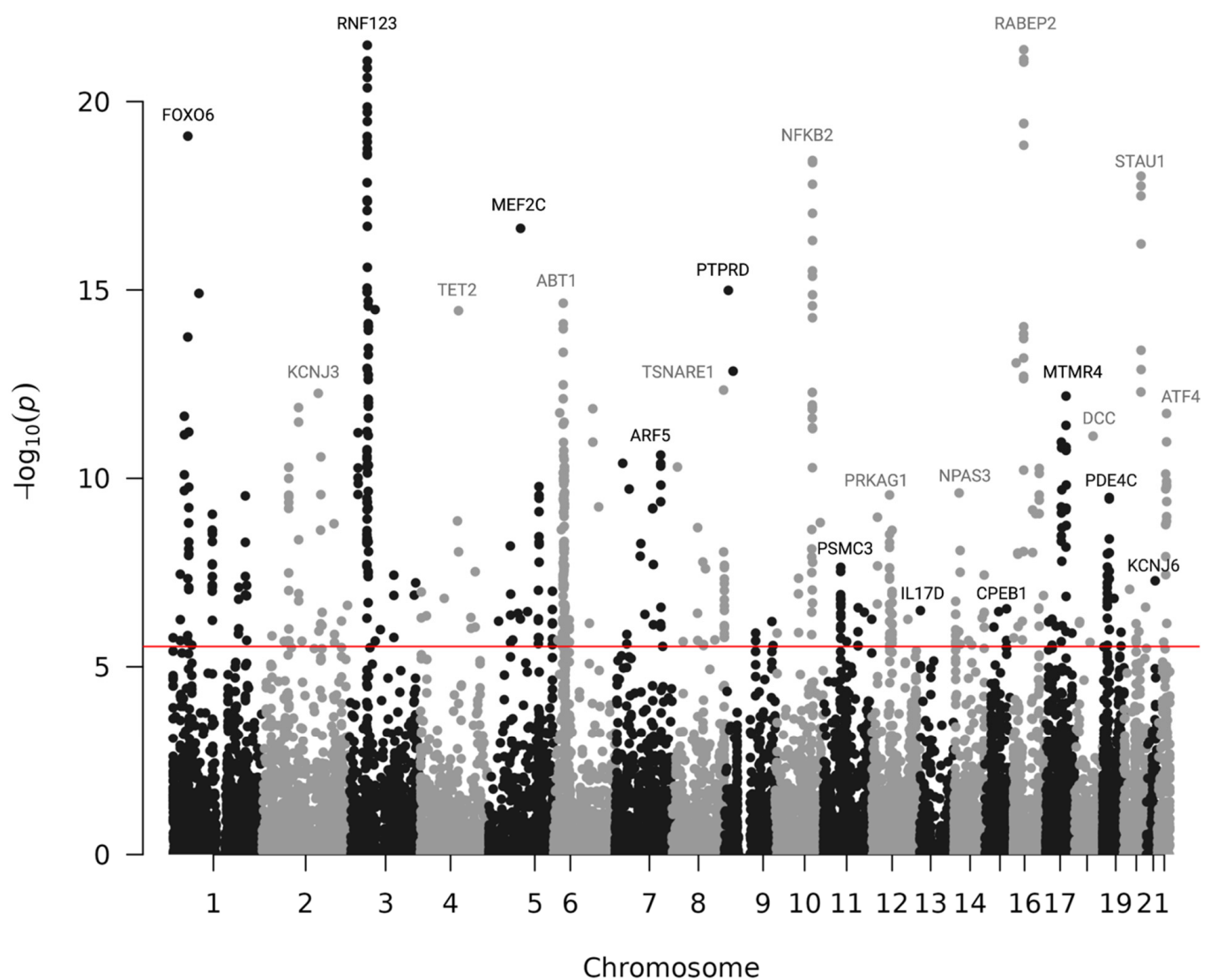(**a**) General cognitive function from the Davies et al. (2018) GWAS

Figure 1. *Cont.*

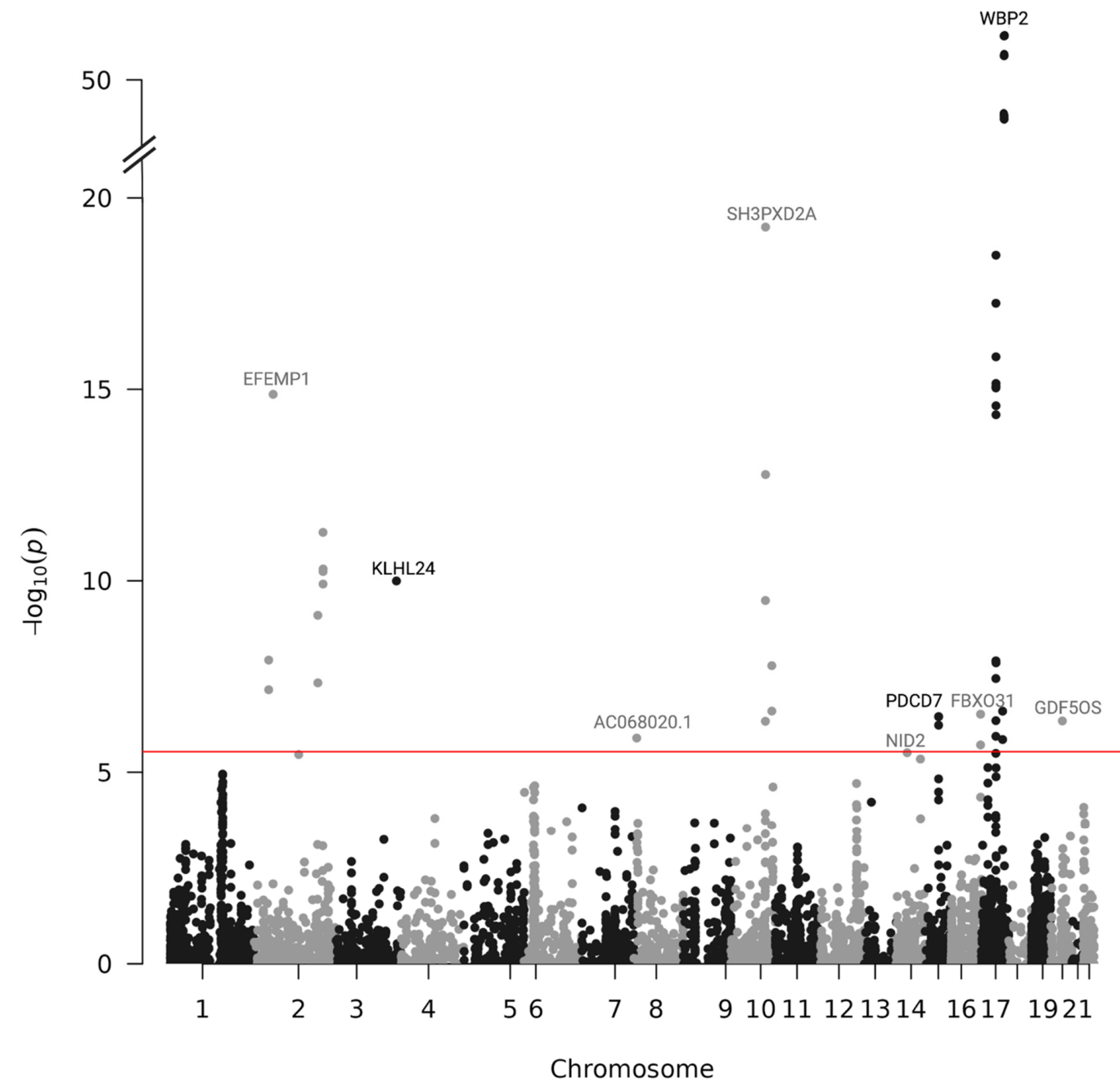(**b**) White matter hyperintensity from the Sargurupremraj et al. (2020) GWAS

Figure 1. *Cont.*

(**c**) Alzheimer's disease from the Bellenguez et al. (2022) GWAS (EA sample)
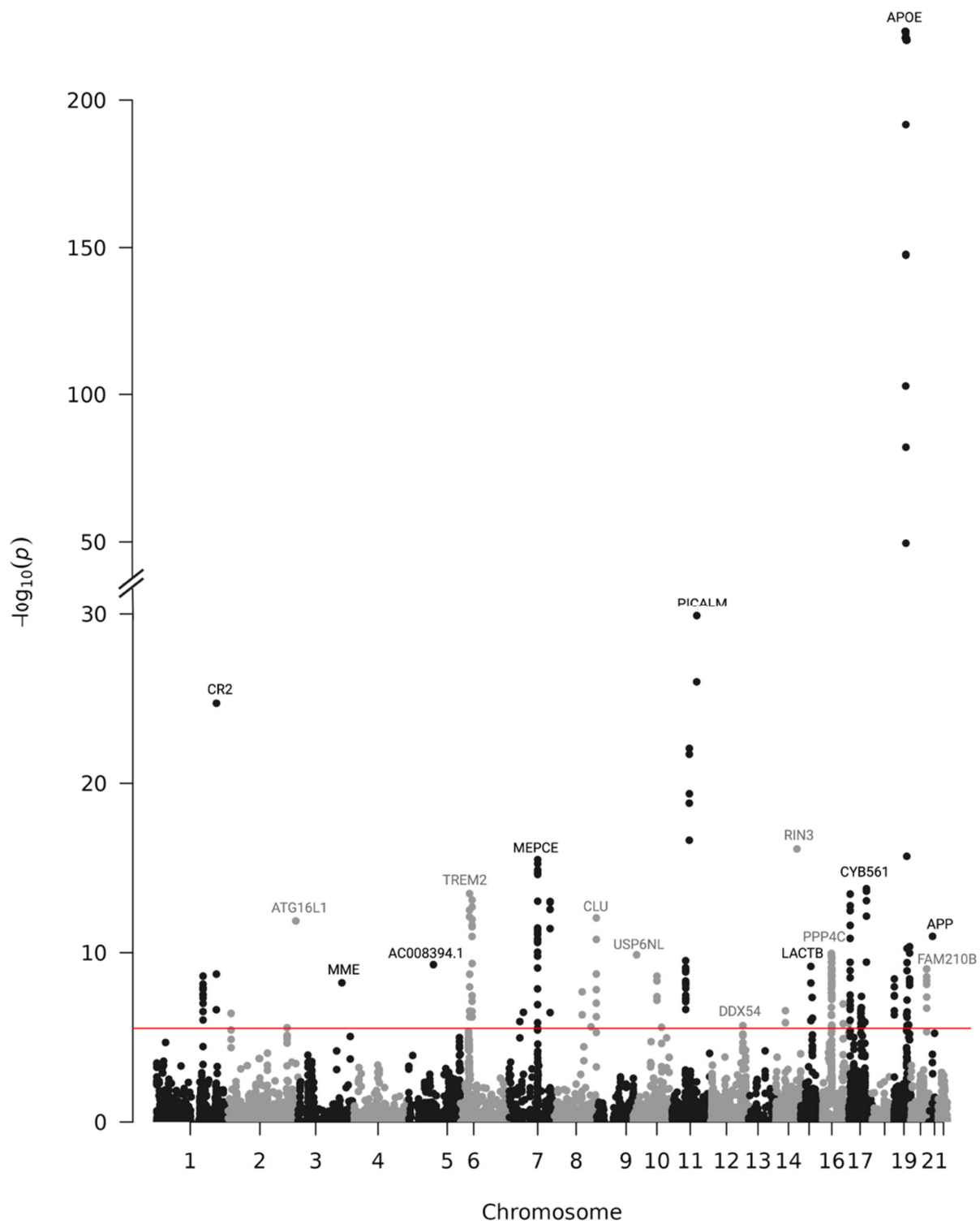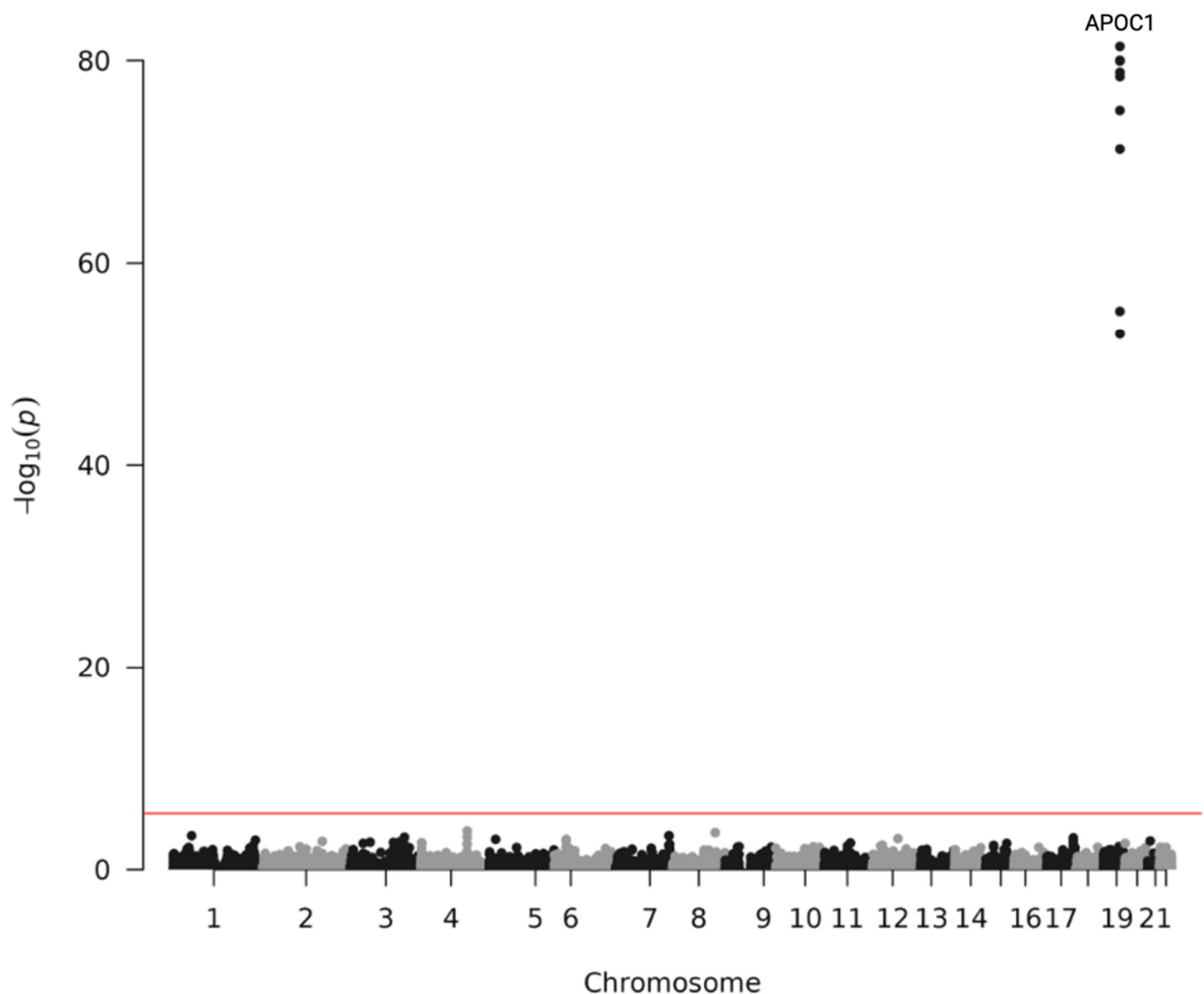

Figure 1. *Cont.*

(**d**) Alzheimer's disease from the Kunkle et al. (2021) GWAS (AA sample)

Figure 1. Manhattan plots of $-\log_{10}$ p-values for gene–trait associations in METRO. Manhattan plots of the association between genes and (**a**) general cognitive function using summary statistics from Davies et al. (2018) [21], (**b**) white matter hyperintensity from Sargurupremraj et al. (2020) [22], (**c**) Alzheimer's disease from Bellenguez et al. (2022) (EA GWAS sample) [23], and (**d**) Alzheimer's disease from Kunkle et al. (2021) (AA GWAS sample) [24] using GENOA gene expression data. The red line indicates significance after Bonferroni correction ($p < 2.90 \times 10^{-6}$).
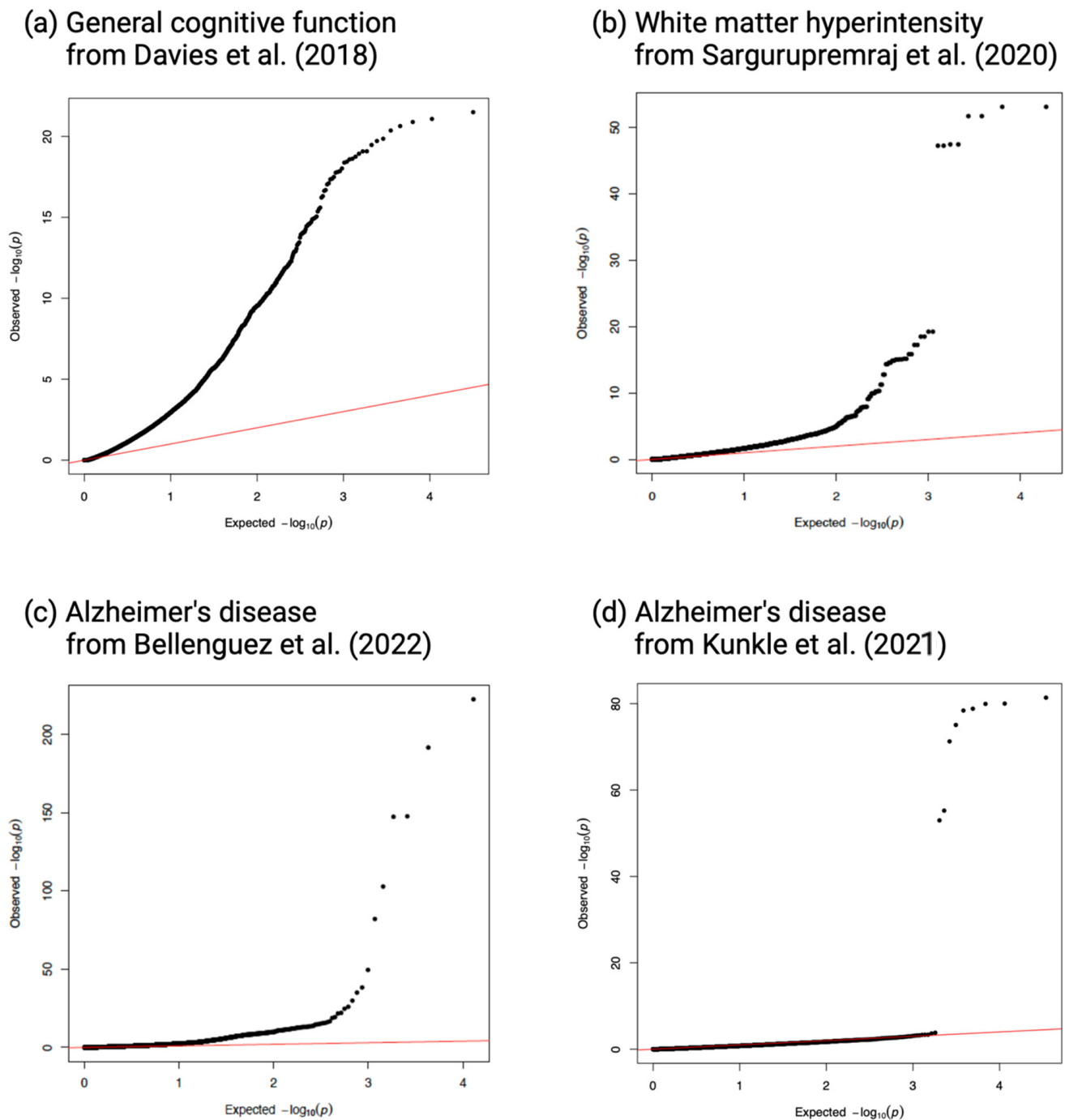
Figure 2. Quantile–quantile (Q-Q) plots of $-\log_{10}$ *p*-values for gene-trait associations in METRO. Q–Q plots of the associations between genes and (**a**) general cognitive function (λ = 2.55) using summary statistics from Davies et al. (2018) [21], (**b**) white matter hyperintensity (λ = 1.45) from Sargurupremraj et al. (2020) [22], (**c**) Alzheimer's disease (λ = 2.09) from Bellenguez et al. (2022) (EA GWAS sample) [23], and (**d**) Alzheimer's disease (λ = 1.0) from Kunkle et al. (2021) (AA GWAS sample) [24] using GENOA gene expression data.
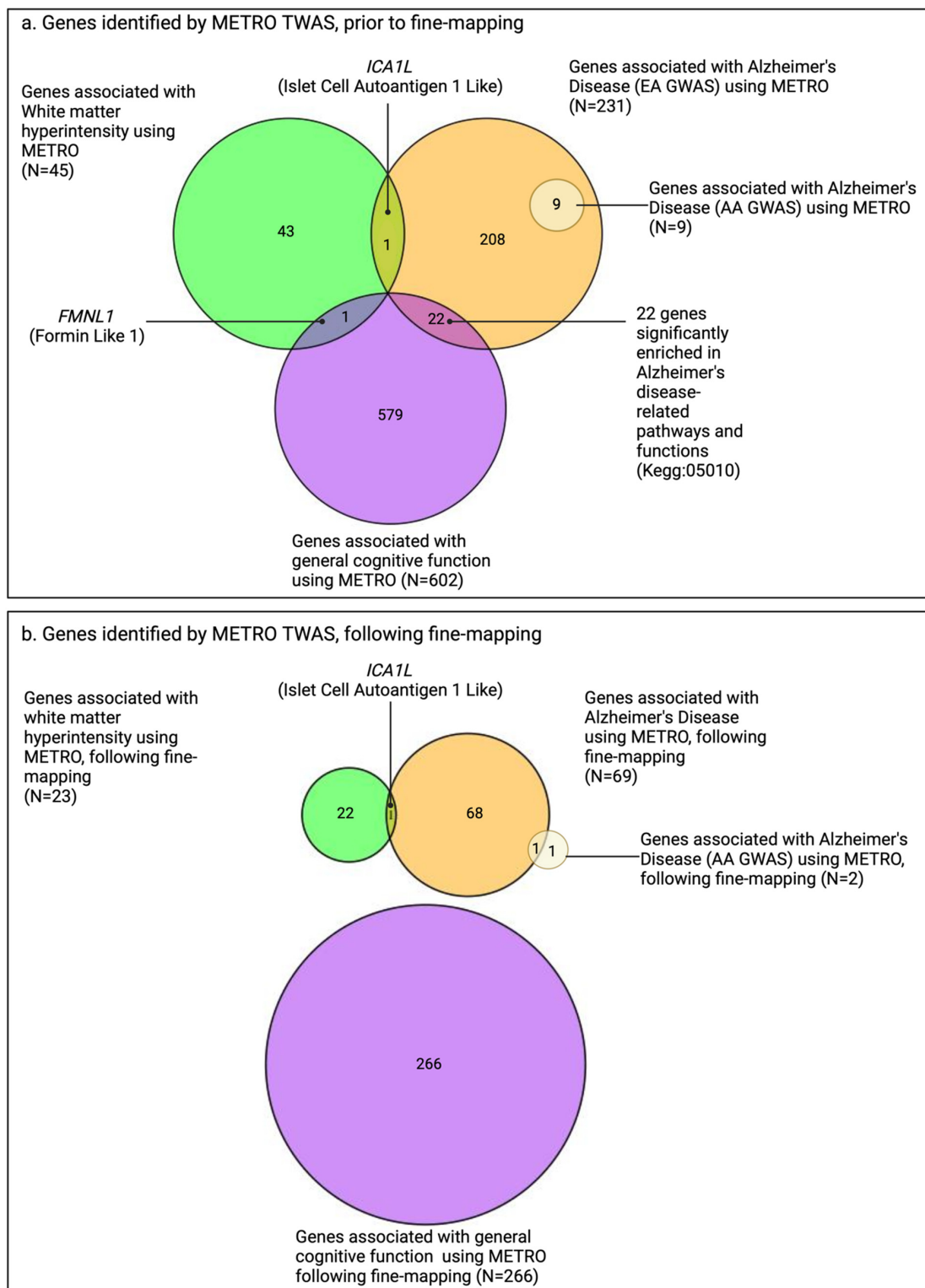
Figure 3. Venn diagrams comparing number of genes associated with general cognitive function, white matter hyperintensity, and Alzheimer's disease (AD) in European ancestry (EA) and AD in African ancestry (AA) using METRO, prior to and following FOCUS fine-mapping. Venn diagrams comparing the number of genes associated with general cognitive function (purple; N = 266 genes), white matter hyperintensity (WMH; green; N = 23 genes), and Alzheimer's disease (AD) in EA (orange; N = 69 genes) and AD in AA (yellow; N = 2 genes), (**a**) prior to fine-mapping and (**b**) following FOCUS [25] fine-mapping using METRO and GENOA expression data after Bonferroni correction ($p < 2.90 \times 10^{-6}$), with GWAS summary statistics obtained from the Davies et al. (2018) [21], Sargurupremraj et al. (2020) [22], Bellenguez et al. (2022) [23], and Kunkle et al. (2021) [24].
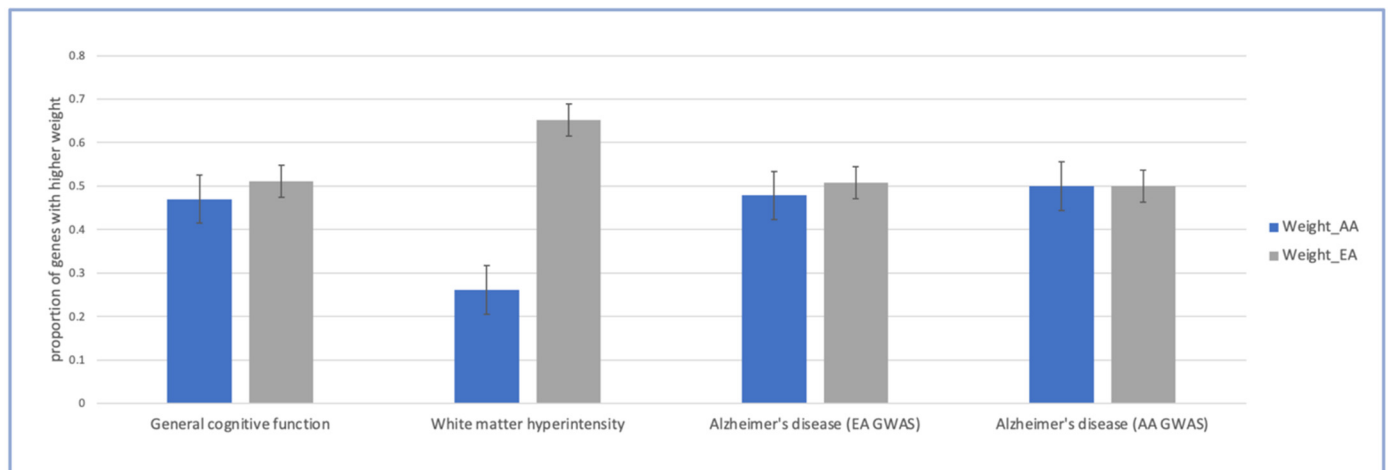
Figure 4. Contribution weights of expression prediction models across all significant fine-mapped genes identified by METRO. Barplots of general cognitive function, white matter hyperintensity, and Alzheimer's disease (AD) in European ancestry (EA) and AD in African ancestry (AA) comparing the proportion of significant genes with higher contribution weights of expression prediction models across all significant genes ($p < 2.90 \times 10^{-6}$). Black bars are the standard errors for the estimated proportions.
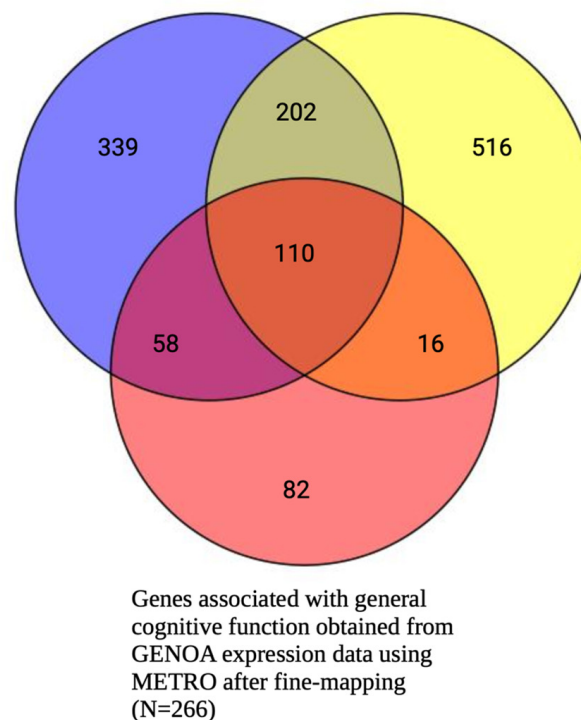
Figure 5. Venn diagram comparing number of METRO-identified genes associated with general cognitive function following FOCUS fine-mapping and genes identified by Davies et al. (2018) gene-based and SNP-based analyses. Venn diagram comparing the number of genes associated with general cognitive function obtained from METRO using GENOA gene expression data after Bonferroni correction ($p < 2.90 \times 10^{-6}$) and FOCUS [25] fine-mapping (red) and Davies et al. (2018) [21]. Davies et al. results included SNP-based association results that were mapped to the nearest gene ($p < 5 \times 10^{-8}$; yellow) and gene-based association results ($p < 2.75 \times 10^{-6}$; blue).
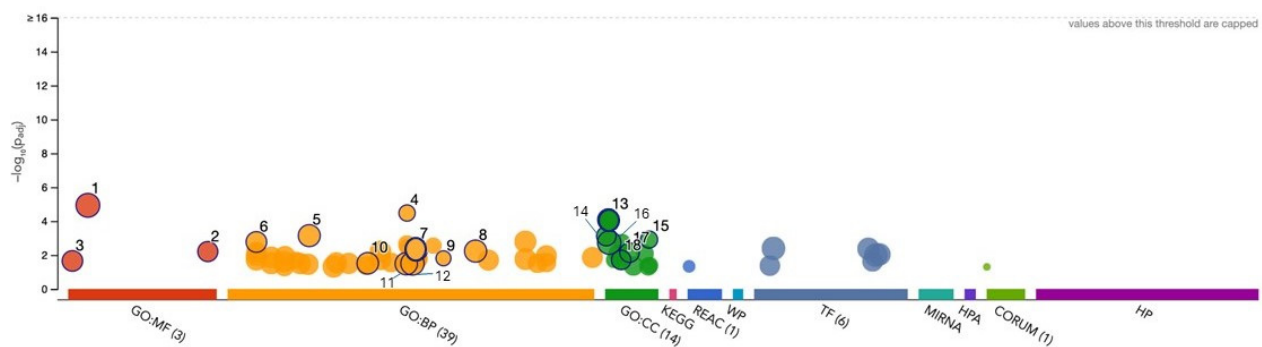
ID	Term ID	Term Name	Adjusted *p*-value
		GO:MF	
1	GO:0005515	Protein binding	1.17×10^{-5}
2	GO:0140110	Transcription regulator activity	6.23×10^{-3}
3	GO:0003677	DNA binding	2.23×10^{-2}
		GO:BP	
4	GO:0048588	Developmental cell growth	3.33×10^{-5}
5	GO:0019538	Protein metabolic process	7.18×10^{-4}
6	GO:0006357	Regulation of transcription by RNA polymerase II	4.79×10^{-3}
7	GO:0051171	Regulation of nitrogen compound metabolic processes	4.79×10^{-3}
8	GO:0080090	Regulation of primary metabolic process	5.86×10^{-3}
9	GO:0061387	Regulation of extent of cell growth	1.56×10^{-2}
10	GO:0042221	Response to chemical	3.06×10^{-2}
11	GO:0050794	Regulation of cellular process	3.13×10^{-2}
12	GO:0048518	Positive regulation of biological process	3.24×10^{-2}
		GO:CC	
13	GO:0005654	Nucleoplasm	8.23×10^{-5}
14	GO:0000785	Chromatin	7.56×10^{-4}
15	GO:0098984	Neuron to neuron synapse	1.22×10^{-3}
16	GO:0005737	Cytoplasm	1.84×10^{-3}
17	GO:0043005	Neuron projection	7.14×10^{-3}
18	GO:0031967	Organelle envelope	1.96×10^{-2}

Figure 6. Functional enrichment analysis on the fine-mapped gene set identified for general cognitive function using METRO TWAS (N = 266 genes). The top panel consists of a Manhattan plot that illustrates the enrichment analysis results. The *x*-axis represents functional terms that are grouped and color-coded by data sources, including Gene Ontology (GO): molecular function (MF; red), GO: biological process (BP; orange), GO: cellular component (CC; dark green), Kyoto Encyclopedia of Genes and Genomes (KEGG; pink), Reactome (REAC; dark blue), WikiPathways (WP; turquoise), Transfac (TF; light blue), MiRTarBase (MIRNA; emerald green), Human Protein Atlas (HPA; dark purple), CORUM protein complexes (light green), and Human Phenotype Ontology (HP; violet), in order from left to right. The *y*-axis shows the adjusted enriched $-\log_{10}$ *p*-values < 0.05. Multiple testing correction was performed using the g:SCS method (Set Counts and Sizes) that takes into account overlapping terms. The top panel highlights driver GO terms identified using the greedy filtering algorithm in g:Profiler. The light circles represent terms that were not significant after filtering. The circle sizes are in accordance with the corresponding term size (i.e., larger terms have larger circles). The number in parentheses following the source name in the *x*-axis shows how many significantly enriched terms were from this source.

After fine-mapping, there were 23 genes in the 90%-credible set across 15 genomic regions for WMH, including 12 genes that were not previously identified in the SNP-based GWAS results mapped to the nearest gene or the gene-based analysis results from Sargurupremraj et al. (2020) [22] (Figure 7, Table S2). Specifically, there were 7 and 12 overlapping genes between METRO and the SNP-based and gene-based associations from Sarguruprem-raj et al. (2020) [22], respectively (Figure 7). The 23 METRO-identified genes were enriched for zinc finger motif ($p_{adj} = 1.27 \times 10^{-2}$), miRNA has-212-5p ($p_{adj} = 1.94 \times 10^{-2}$), and the retinal inner plexiform layer ($p_{adj} = 3.86 \times 10^{-2}$; Figure 8). The 12 genes associated with WMH that were previously not identified by Sargurupremraj et al. (2020) [22] were enriched for DNA binding domain Zinc Finger Protein 690 (ZNF690; $p_{adj} = 2.52 \times 10^{-3}$) and the ClpX protein degradation complex ($p_{adj} = 4.97 \times 10^{-2}$; Figure S3).
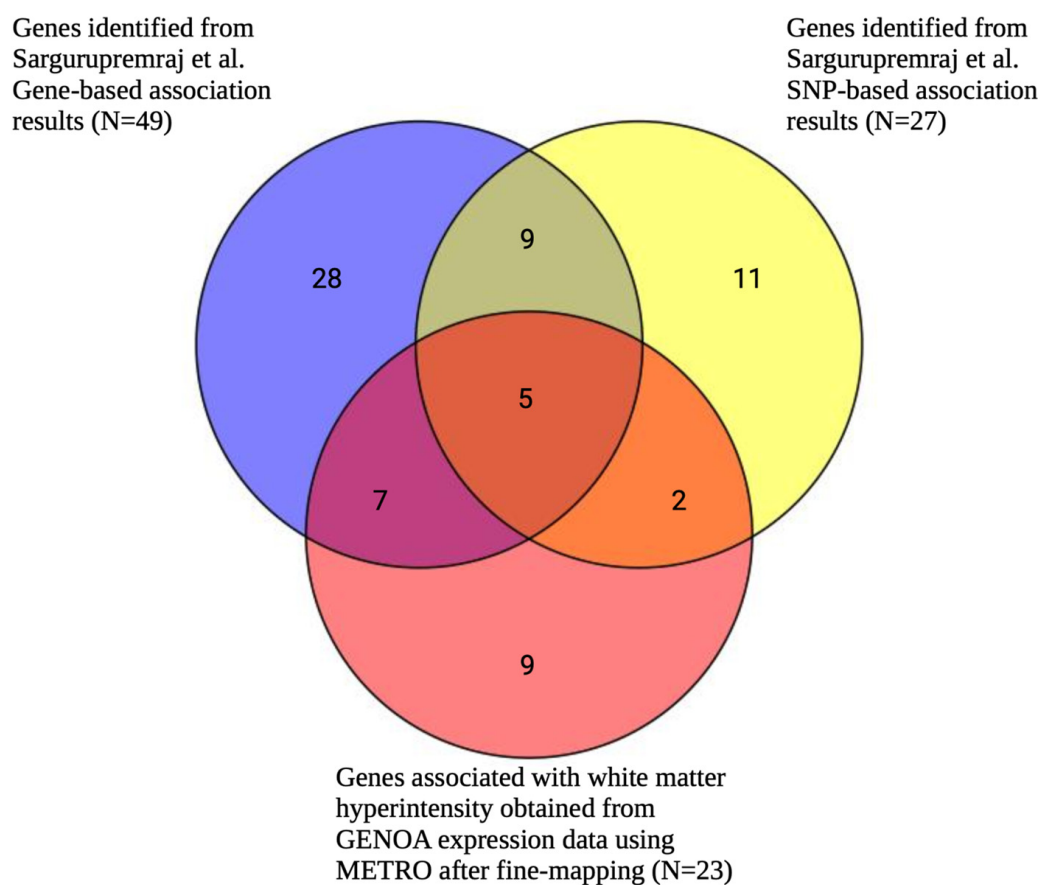
Figure 7. Venn diagram comparing number of METRO-identified genes associated with white matter hyperintensity following FOCUS fine-mapping and genes identified by Sargurupremraj et al. (2020) gene-based and SNP-based analyses. Venn diagram comparing the number of significantly associated genes associated with white matter hyperintensity (WMH) obtained from METRO using GENOA expression data after Bonferroni correction ($p < 2.90 \times 10^{-6}$) and fine-mapping (red) and Sargurupremraj et al. (2020) [22]. Sargurupremraj et al.'s results included SNP-based association results that were mapped to the nearest gene ($p < 5 \times 10^{-8}$; yellow) and gene-based association results ($p < 2.77 \times 10^{-6}$; blue).

ID	Term ID	Term Name	Adjusted *p*-value
		TF	
1	TF:M12713	Factor: ZNF690; motif: GTCTACRCNG	1.27×10^{-2}
		MIRNA	
2	MIRNA: has-miR-212-5p	hsa-miR-212-5p	1.94×10^{-2}
		HPA	
3	HPA:0411242	Retina; inner plexiform layer [≥Medium]	3.86×10^{-2}

Figure 8. Functional enrichment analysis on the fine-mapped gene set identified for white matter hyperintensity using METRO TWAS (N = 23 genes). The top panel consists of a Manhattan plot that illustrates the enrichment analysis results. The *x*-axis represents functional terms that are grouped and color-coded by data sources, including Gene Ontology (GO): molecular function (MF; red), GO: biological process (BP; orange), GO: cellular component (CC; dark green), Kyoto Encyclopedia of Genes and Genomes (KEGG; pink), Reactome (REAC; dark blue), WikiPathways (WP; turquoise), Transfac (TF; light blue), MiRTarBase (MIRNA; emerald green), Human Protein Atlas (HPA; dark purple), CORUM protein complexes (light green), and Human Phenotype Ontology (HP; violet), in order from left to right. The *y*-axis shows the adjusted enriched $-\log_{10}$ *p*-values < 0.05. Multiple testing correction was performed using the g:SCS method (Set Counts and Sizes) that takes into account overlapping terms. The top panel highlights driver GO terms identified using the greedy filtering algorithm in g:Profiler. The light circles represent terms that were not significant after filtering. The circle sizes are in accordance with the corresponding term size (i.e., larger terms have larger circles). The number in parentheses following the source name in the *x*-axis shows how many significantly enriched terms were from this source.

After fine-mapping, there were 69 genes in the 90%-credible set across 56 genomic regions associated with AD (EA GWAS), including 45 genes that were not previously identified in the SNP-based GWAS results mapped to the nearest gene or the gene prioritization analysis results from Bellenguez et al. (2022) [23] (Figure 9, Table S3). Specifically, there were 16 and 14 overlapping genes between METRO and the SNP-based and gene prioritization test results from Bellenguez et al. (2022) [23], respectively (Figure 9). The 69 METRO-identified genes were enriched for AD-associated processes, including the regulation of amyloid fibril formation ($p_{adj} = 1.87 \times 10^{-3}$), amyloid-beta clearance ($p_{adj} = 1.90 \times 10^{-3}$), microglial cell activation ($p_{adj} = 5.79 \times 10^{-3}$), the amyloid-beta metabolic process ($p_{adj} = 1.07 \times 10^{-2}$), and neurofibrillary tangles ($p_{adj} = 2.80 \times 10^{-4}$; Figure 10). The 45 genes associated with AD that were previously not identified by Bellenguez et al. (2022) [23] were enriched for hematopoietic cell lineage ($p_{adj} = 1.73 \times 10^{-3}$) and neurofibrillary tangles ($p_{adj} = 9.13 \times 10^{-3}$; Figure S4).
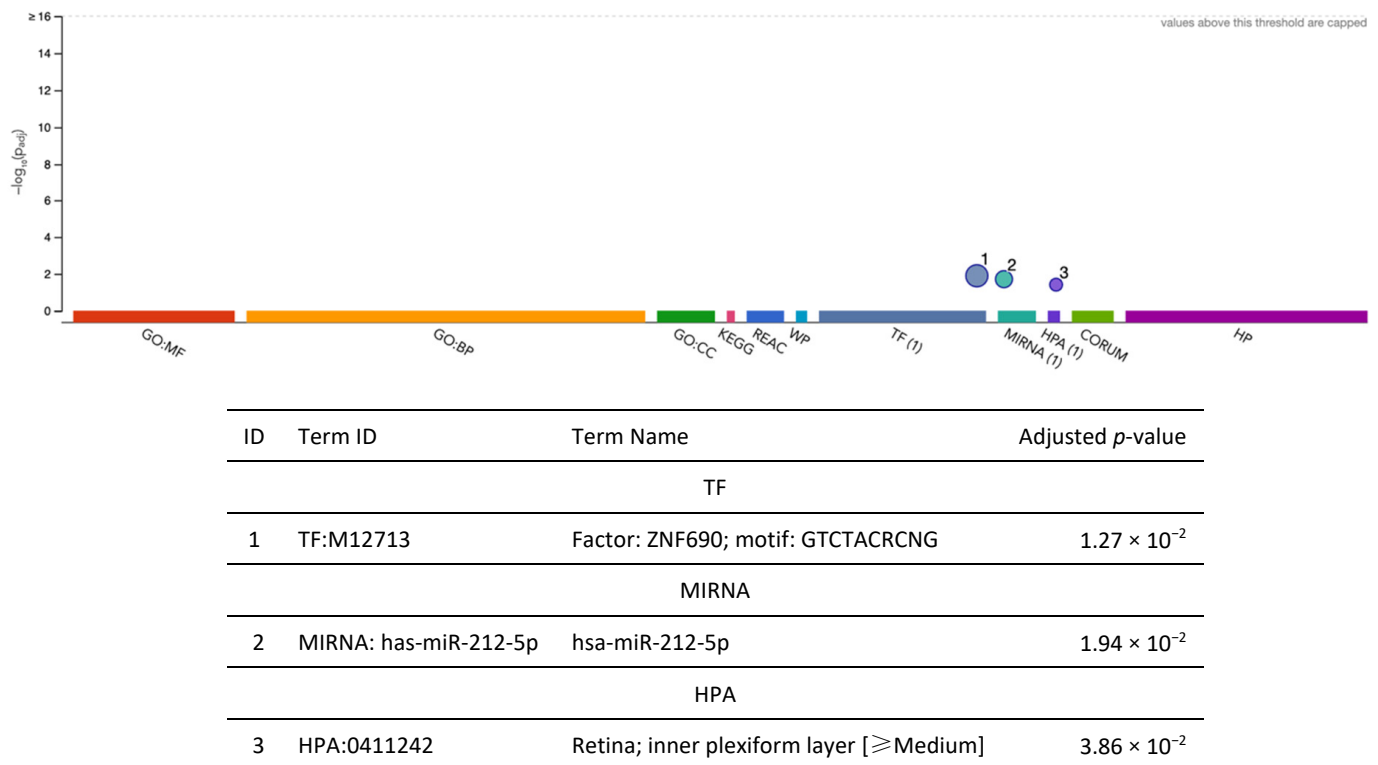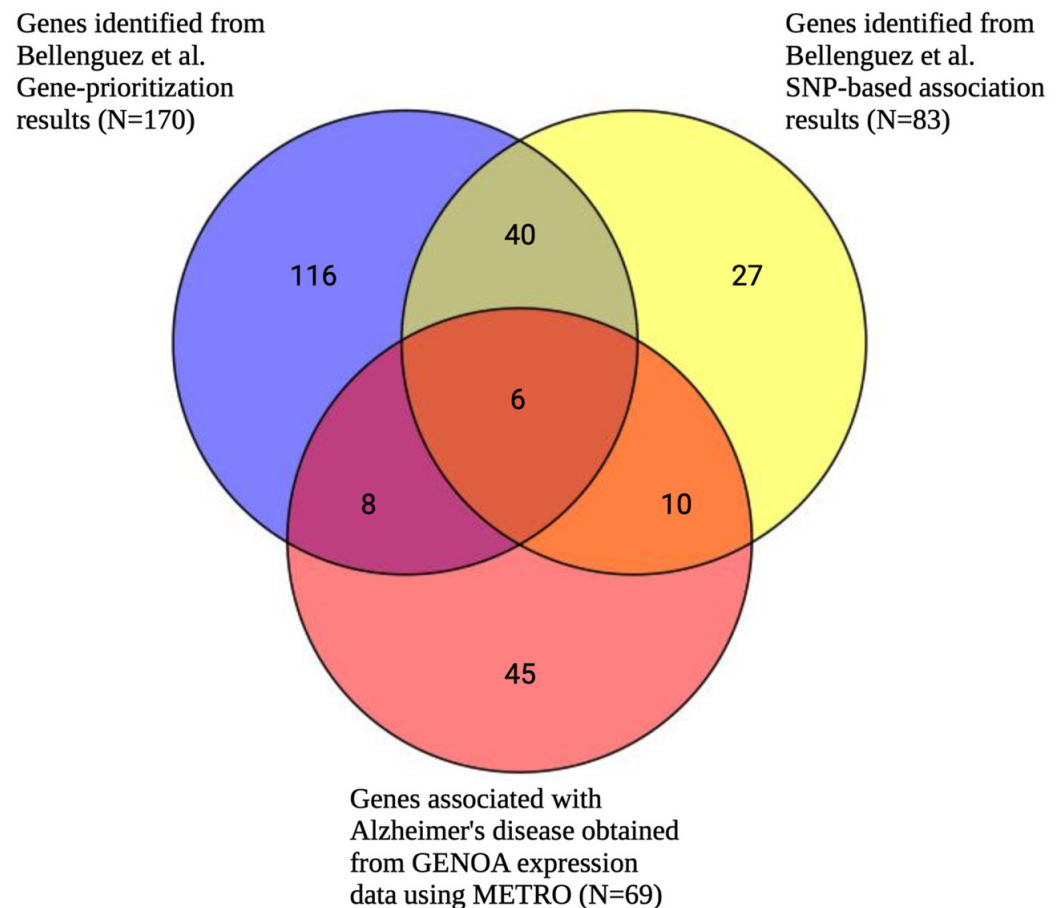
Figure 9. Venn diagram comparing number of METRO-identified genes associated with Alzheimer's disease (EA GWAS) following FOCUS fine-mapping and genes identified by Bellenguez et al. (2022) gene prioritization and SNP-based analyses. Venn diagram comparing the number of significantly associated genes associated with Alzheimer's disease (from EA GWAS) obtained from METRO using GENOA expression data after Bonferroni correction ($p < 2.90 \times 10^{-6}$) and fine-mapping (red) and Bellenguez et al. (2022) [23]. Bellenguez et al.'s results included SNP-based association results that were mapped to the nearest gene ($p < 5 \times 10^{-8}$; yellow) and gene prioritization results for the genes in the novel AD risk loci (blue). In the gene prioritization analysis, Bellenguez et al. analyzed the downstream effects of new AD-associated loci on molecular phenotypes (i.e., expression, splicing, protein expression, methylation, and histone acetylation) in various *cis*-quantitative trait loci (*cis*-QTL) catalogues from AD-relevant tissues, cell types, and brain regions.

We identified 2 genes, *TOMM40* ($\alpha = 10.02$; $p = 1.15 \times 10^{-80}$) and *PVRL2* ($\alpha = -10.72$; $p = 9.67 \times 10^{-81}$), in the 90%-credible set associated with AD (AA GWAS) (Table S4). After fine-mapping, none of these genes overlapped with the SNP-based GWAS results mapped to the nearest gene or the gene-based analysis results from Kunkle et al. (2021) [24], since they were both in the broader *APOE* region, which was the only identified gene in Kunkle et al. (2021) [24]. The two METRO-identified genes were enriched for coreceptor-mediated virion attachment to a host ($p_{adj} = 4.96 \times 10^{-2}$; Figure 11).

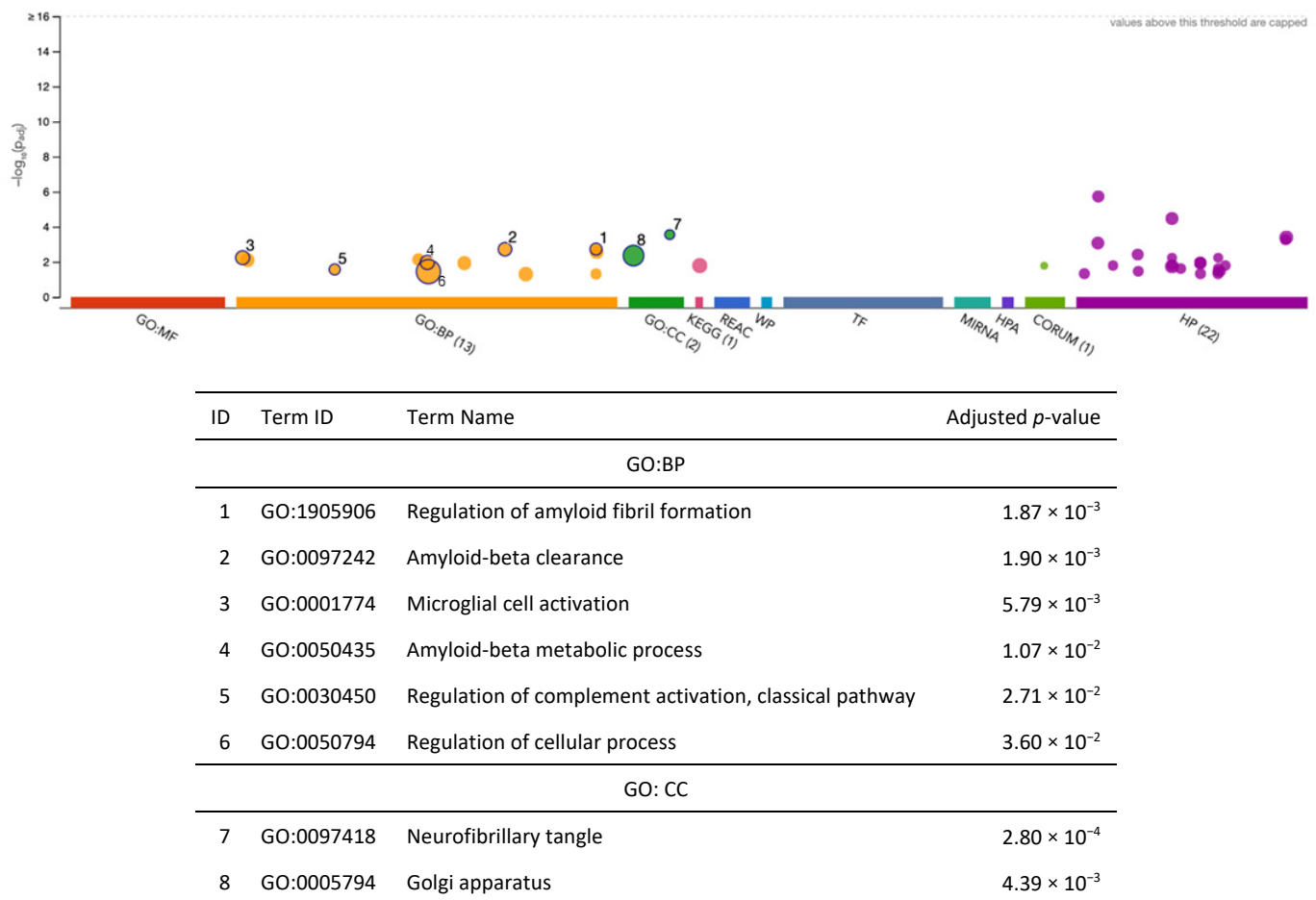| ID	Term ID	Term Name	Adjusted *p*-value
		GO:BP	
1	GO:1905906	Regulation of amyloid fibril formation	1.87×10^{-3}
2	GO:0097242	Amyloid-beta clearance	1.90×10^{-3}
3	GO:0001774	Microglial cell activation	5.79×10^{-3}
4	GO:0050435	Amyloid-beta metabolic process	1.07×10^{-2}
5	GO:0030450	Regulation of complement activation, classical pathway	2.71×10^{-2}
6	GO:0050794	Regulation of cellular process	3.60×10^{-2}
		GO: CC	
7	GO:0097418	Neurofibrillary tangle	2.80×10^{-4}
8	GO:0005794	Golgi apparatus	4.39×10^{-3}

Figure 10. Functional enrichment analysis on the fine-mapped gene set identified for Alzheimer's disease (EA GWAS) using METRO TWAS (N = 69 genes). The top panel consists of a Manhattan plot that illustrates the enrichment analysis results. The *x*-axis represents functional terms that are grouped and color-coded by data sources, including Gene Ontology (GO): molecular function (MF; red), GO: biological process (BP; orange), GO: cellular component (CC; dark green), Kyoto Encyclopedia of Genes and Genomes (KEGG; pink), Reactome (REAC; dark blue), WikiPathways (WP; turquoise), Transfac (TF; light blue), MiRTarBase (MIRNA; emerald green), Human Protein Atlas (HPA; dark purple), CORUM protein complexes (light green), and Human Phenotype Ontology (HP; violet), in order from left to right. The *y*-axis shows the adjusted enriched $-\log_{10}$ *p*-values < 0.05. Multiple testing correction was performed using the g:SCS method (Set Counts and Sizes) that takes into account overlapping terms. The top panel highlights driver GO terms identified using the greedy filtering algorithm in g:Profiler. The light circles represent terms that were not significant after filtering. The circle sizes are in accordance with the corresponding term size (i.e., larger terms have larger circles). The number in parentheses following the source name in the *x*-axis shows how many significantly enriched terms were from this source.

We compared the genes identified by METRO before and after fine-mapping with those identified by the TWASs in Sargurupremraj et al. (2020) [22] and Bellenguez et al. (2022) [23], which used TWAS-Fusion (Figure 12). For WMH, there were 16 and 10 genes identified both by METRO before and after fine-mapping and by the TWAS-Fusion analysis conducted by Sargurupremraj et al. (2020) [22], respectively (Table 2). For AD, there were 24 and 10 genes identified both by METRO before and after fine-mapping and by the TWAS-Fusion followed by FOCUS fine-mapping analysis conducted by Bellenguez et al. (2022) [23] (Table 3). *ICA1L* was the only gene overlapping between the AD and WMH TWAS association results.
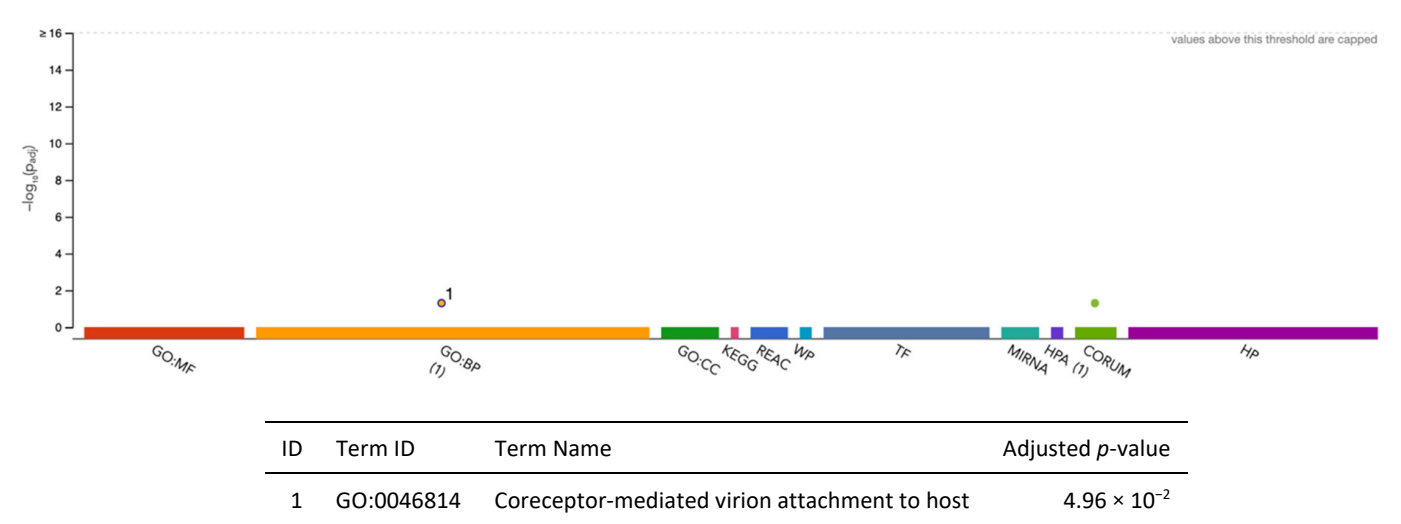
ID	Term ID	Term Name	Adjusted *p*-value
1	GO:0046814	Coreceptor-mediated virion attachment to host	4.96×10^{-2}

Figure 11. Functional enrichment analysis fine-mapped gene set identified for Alzheimer's disease (AA GWAS) using METRO TWAS (N = 2 genes). The top panel consists of a Manhattan plot that illustrates the enrichment analysis results. The *x*-axis represents functional terms that are grouped and color-coded by data sources, including Gene Ontology (GO): molecular function (MF; red), GO: biological process (BP; orange), GO: cellular component (CC; dark green), Kyoto Encyclopedia of Genes and Genomes (KEGG; pink), Reactome (REAC; dark blue), WikiPathways (WP; turquoise), Transfac (TF; light blue), MiRTarBase (MIRNA; emerald green), Human Protein Atlas (HPA; dark purple), CORUM protein complexes (light green), and Human Phenotype Ontology (HP; violet), in order from left to right. The *y*-axis shows the adjusted enriched $-\log_{10}$ *p*-values < 0.05. Multiple testing correction was performed using the g:SCS method (Set Counts and Sizes) that takes into account overlapping terms. The top panel highlights driver GO terms identified using the greedy filtering algorithm in g:Profiler. The light circles represent terms that were not significant after filtering. The circle sizes are in accordance with the corresponding term size (i.e., larger terms have larger circles). The number in parentheses following the source name in the *x*-axis shows how many significantly enriched terms were from this source.

Table 2. Genes for WMH identified both by METRO followed by fine-mapping with FOCUS and by TWAS-Fusion conducted by Sargurupremraj et al. (2020) [22].

Gene	ENSG	Chr	Start	End	Gene Name	Accession Number (HGNC ID)
CALCRL	ENSG00000064989	2	188206691	188313187	Calcitonin receptor like receptor	HGNC:16709
DCAKD	ENSG00000172992	17	43100706	43138499	Dephospho-CoA kinase domain containing	HGNC:26238
EFEMP1	ENSG00000115380	2	56093102	56151274	EGF containing fibulin extracellular matrix protein 1	HGNC:3218
GJC1	ENSG00000182963	17	42875816	42908184	Gap junction protein gamma 1	HGNC:4280
ICA1L	ENSG00000163596	2	203637873	203736489	Islet cell autoantigen 1 like	HGNC:14442
KLHL24	ENSG00000114796	3	183353398	183402307	Kelch like family member 24	HGNC:25947
NBEAL1	ENSG00000144426	2	203879331	204091101	Neurobeachin like 1	HGNC:20681
NEURL	ENSG00000107954	10	105253462	105352303	Neuralized E3 ubiquitin protein ligase 1	HGNC:7761
NMT1	ENSG00000136448	17	43035360	43186384	N-myristoyltransferase 1	HGNC:7857
WBP2	ENSG00000132471	17	73841780	73852588	WW domain binding protein 2	HGNC:12738

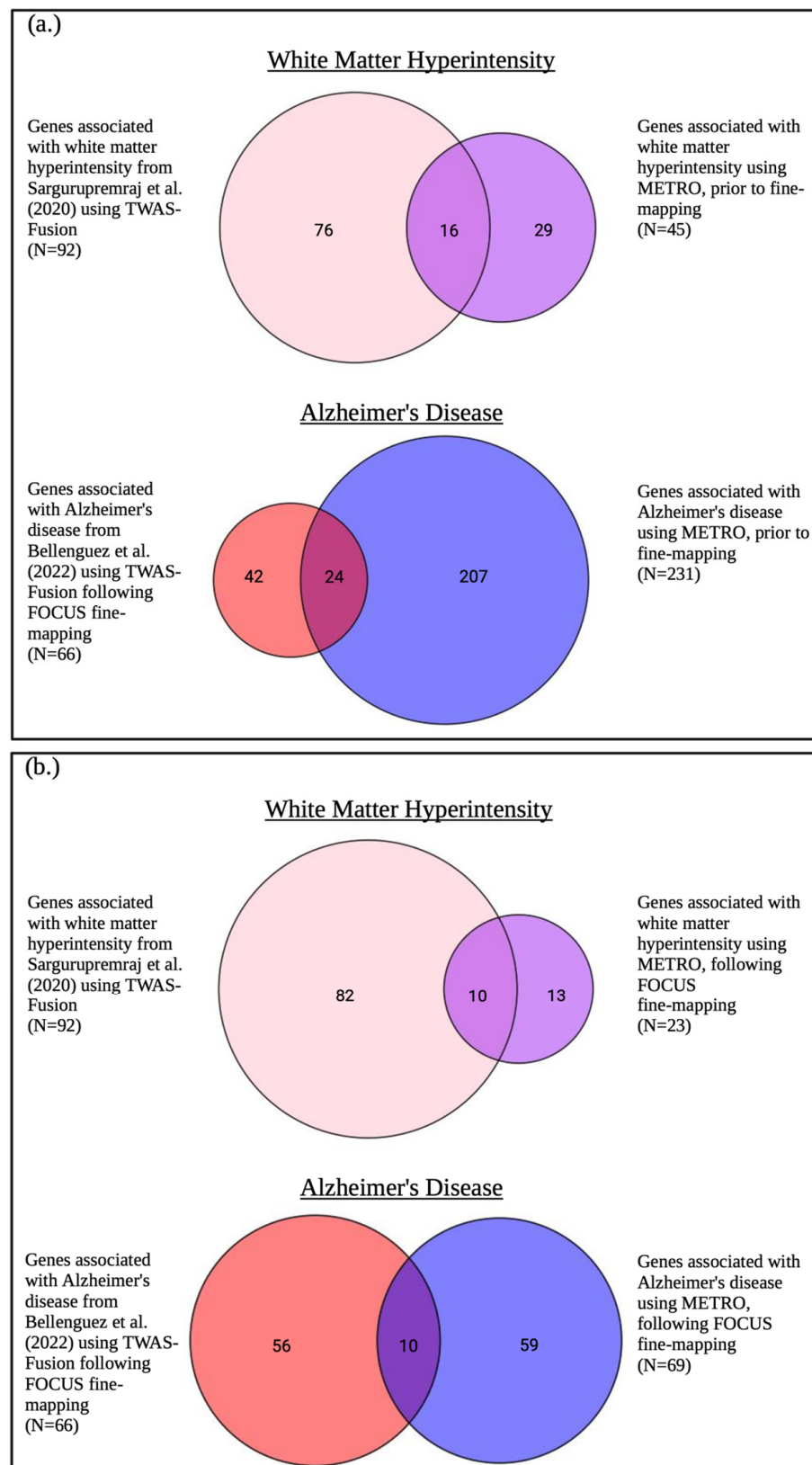Abbreviations: HGNC, Human Genome Organisation Gene Nomenclature Committee.

Figure 12. Venn diagram comparing METRO TWAS results prior to and following FOCUS fine-mapping with TWAS results from Sargurupremraj et al. (2020) and Bellenguez et al. (2022). Venn diagram comparing METRO TWAS results (**a**) prior to and (**b**) following FOCUS [25] fine-mapping with TWAS results using Fusion for white matter hyperintensity from Sargurupremraj et al. [22] (2020) without fine-mapping and Alzheimer's disease from Bellenguez et al. [23] (2022) (EA GWAS) with FOCUS fine-mapping.

Table 3. Genes for AD identified both by METRO followed by fine-mapping with FOCUS and by TWAS-Fusion followed by fine-mapping with FOCUS conducted by Bellenguez et al. (2022) [23].

Gene	ENSG	Chr	Start	End	Gene Name	Accession Number (HGNC ID)
BLNK	ENSG00000095585	10	97948927	98031344	B cell linker	HGNC:14211
CPSF3	ENSG00000119203	2	9563780	9613230	Cleavage and polyadenylation specific factor 3	HGNC:2326
DDX54	ENSG00000123064	12	113594978	113623284	DEAD-box helicase 54	HGNC:20084
GRN	ENSG00000030582	17	42422614	42430474	Granulin precursor	HGNC:4601
ICA1L	ENSG00000163596	2	203637873	203736489	Islet cell autoantigen 1 like	HGNC:14442
KLF16	ENSG00000129911	19	1852398	1863578	KLF transcription factor 16	HGNC:16857
LACTB	ENSG00000103642	15	63414032	63434260	Lactamase beta	HGNC:16468
PPP4C	ENSG00000149923	16	30087299	30096697	Protein phosphatase 4 catalytic subunit	HGNC:9319
SHARPIN	ENSG00000179526	8	145153536	145163027	SHANK associated RH domain interactor	HGNC:25321
TBX6	ENSG00000149922	16	30097114	30103245	T-box transcription factor 6	HGNC:11605

Abbreviations: HGNC, Human Genome Organisation Gene Nomenclature Committee.

3. Discussion

While previous studies have identified genes associated with cognitive function, WMH, and AD, there are few TWASs that have utilized genetic and gene expression data from multiple ancestries to increase the power to elucidate the gene–trait associations and molecular mechanisms underlying the etiologies of cognitive function and neurocognitive disorders. Using the METRO method in a GWAS consisting primarily of EA samples followed by FOCUS fine-mapping, we identified 266, 23, and 69 genes associated with general cognitive function, WMH, and AD, respectively, with 82, 12, and 45 of them not previously identified in the original GWAS. In addition, using an AA GWAS, we identified two fine-mapped genes associated with AD, both of which were proximal to *APOE*. Studying the gene expression mechanisms underlying cognitive function, WMH, and dementia using both EA and AA expression data may enhance our understanding of cognitive health prior to and following the onset of dementia and further allow us to generalize the findings from large-scale EA GWASs to other ancestries.

AD and SVD have overlapping features that contribute to dementia neuropathology, including the breakdown of the blood–brain barrier [26] and the presence of small cortical and subcortical infarcts, microbleeds, perivascular spacing, and WMH in brain tissue [27]. After fine-mapping, Islet Cell Autoantigen 1 Like (*ICA1L*) was identified in both the WMH and AD TWASs. This is a highly plausible prioritized gene that is likely to modulate the metabolism of amyloid precursor protein (APP) [23] and increase the risk of AD. *ICA1L* encodes a protein whose expression is activated by type IV collagen and plays a crucial role in myelination [28]. Increased *ICA1L* expression is also associated with a lower risk of AD [29–31] and small vessel strokes (SVSs), the acute outcomes of cerebral SVD, which may lead to VaD [32]. Consistent with these studies, our TWAS found that a decreased expression of *ICA1L* is associated with an increased risk of AD and WMH, a subclinical indicator of SVD. Single-cell RNA-sequencing has shown *ICA1L* expression to be enriched in cortical glutamatergic excitatory neurons, which are crucial components in neural development and neuropathology through their roles in cell proliferation, differentiation, survival, neural network formation and cell death [33,34]. *ICA1L* has been examined as a possible drug target for SVD, AD, and other neurodegenerative diseases [32,35]; however, it is not recommended as a prioritized drug at this time due to potential side effects, including an increased risk of coronary artery disease and myocardial infarction, as well as a lower diastolic blood pressure [35]. Nevertheless, future research could validate *ICA1L* as a biomarker through longitudinal studies assessing its levels in cerebrospinal fluid and blood, investigating its ability to cross the blood–brain barrier, and characterizing how it

correlates with dementia-related outcomes [36–39]. For instance, as both SVD and AD are associated with blood–brain barrier dysfunction, *ICA1L*'s protective effect could potentially be mediated through blood–brain-barrier-related mechanisms [36–39]. As such, further investigation of *ICA1L* and imaging of the blood–brain barrier may allow for a greater understanding of this gene as a therapeutic target. As such, *ICA1L* may contribute to overlapping AD and VaD neuropathology, and it could be a potential target for therapeutics and/or preventative treatments for AD and VaD in the future if adverse events can be reduced.

Our TWAS of AD (from the EA GWAS) identified 45 genes that were not identified in the SNP-based GWAS results mapped to the nearest gene or the gene-based analysis reported in Bellenguez et al. (2022) [23]. The 45 genes were enriched for hematopoietic cell lineages, which are progenitors of red and white blood cells, including those related to immunity (e.g., natural killer cells, T- and B-lymphocytes, and other types of leukocytes) [40–46]. Our TWAS identified genes that have been previously associated with AD, including *APOE*, *TOMM40*, *APOC4*, *CLU*, *PICALM*, and *CR2*, among others [23,47,48]. While we identified *APOE*, the strongest genetic risk factor for AD in most populations, after fine-mapping, we did not identify *ABCA7*, which confers an equal or even greater risk for AD in AA individuals [49–51]. This finding is perhaps not surprising considering that our TWAS was conducted using an EA GWAS, and the strength of association between *ABCA7* and AD is comparatively weaker in EA samples than in AA ones [51]. To identify genes associated with AD risk in AA populations, specifically, it would be beneficial to perform a TWAS utilizing a well-powered AD GWAS in AA individuals.

Our TWAS of AD (from the AA GWAS) [24] identified only *TOMM40* and *PVRL2*, both proximal to *APOE*. *TOMM40* was also identified in our TWAS of AD (from the EA GWAS), as well as other AD GWASs [23,47,48]. *PVRL2* has been associated with metabolic syndrome, diabetic dyslipidemia, and AD [52,53]. One study found that polymorphisms in *PVRL2* interact with variants in *TOMM40* to increase AD risk through pathways related to amyloid-beta metabolism in older Chinese adults [53]. As larger AD GWASs in AA populations become available, we may be able to identify additional genes associated with this disease while leveraging gene expression data from EA and AA samples.

In our AD EA TWAS, we also identified genes associated with other neurological and autoimmune diseases, including Parkinson's disease (*CYB561* [54] and *SLC25A39* [55]), Crohn's disease (*ATG16L1* [56]), Amyotrophic lateral sclerosis (*SIGLEC9* [57]), and Riboflavin Transport Deficiency (*SLC52A1* [58]). These diseases have in common the progressive peripheral and cranial degeneration of neurons that impact processes such as voluntary muscle movement, vision, hearing, and sensation. Although not explicitly identified in Bellenguez et al. (2022) [23], we also identified genes that were associated with AD in other studies, including *RIN3* that is implicated in tau-mediated pathology, the *MS4A* (*4A* and *6A*) locus associated with mast cell activation, *TP53INP1* and *ZYX* that have been linked to myeloid enhancer activity [59], and *APOC4*, which is located proximal to *APOE* [60]. We also identified additional genes involved in B cell autoimmunity (*HLA-DQA2* [61,62] and *CSTF1* [63]), neurodegenerative processes (*SUPT4H1* [64], *C6orf10* [65], *IKZF1* [66], and *DEDD* [67]), and neuronal growth (*IKZF1* [66] and *STYX* [68]). Our findings support the hypothesis that the chronic activation of immune cells resident in the brain and peripheral nervous system appears to play a critical role in neuroinflammatory responses that drive the progression of neurodegeneration in AD [69]. Further, consistent with findings that AD and VaD often co-exist, our AD TWAS identified genes that were associated with lacunar and ischemic strokes, as well as cerebral small vessel disease in other studies, including *SLC39A13* [70], *RAPSN* [70], *MAF1* [71], and *MME* [72,73].

Although our WMH TWAS identified 12 genes that were not included in the SNP-based GWAS results mapped to the nearest gene or the gene-based analysis reported in Sargurupremraj et al. (2020) [22], other studies found associations between *MAP1LC3B* [74], *ARMS2* [75,76], and *HTRA1* [70] with ischemic stroke, lacunar stroke, and cerebral SVD. The WMH TWAS also identified genes associated with AD (*ARMS2*) [77], atrial fibrillation (*NEURL* [78] and *GJC1* [79]), innate immunity (*EFTUD2* [80]), and apoptosis and neurodevelopment (*PDCD7* [81], *FBXO31* [82], and *ClpX* [83]). The 12 unique genes identified for WMH were enriched for DNA-binding domain Zinc Finger Protein 690 [84], which plays an essential role in gene regulation, transcription, and various cellular processes, and the ClpX protein degradation complex [85], which maintains protein homeostasis. Our findings are consistent with studies that have shown neuroinflammation to be an immunological cascade reaction by glial cells of the central nervous system, where innate immunity resides.

While our TWAS for general cognitive function did not show overlapping genes between the TWAS for AD and VaD, we identified genes associated with general cognitive function that were not explicitly identified by Davies et al. (2018) [21] which were associated with pre-clinical AD and VaD risk factors, including cardiovascular diseases, immunity, and Alzheimer's neuropathology. Our TWAS also identified genes previously associated with cognitive domains, neuropathology, and psychiatric illness, including reading-related skills and neural structures (*SEMA6D* [86] and *SETBP1* [87]), working memory tasks (*CDH13* [88]), and Schizophrenia (*HP* [89,90], *C18orf1* [91], and *TMEM180* [92]). There are likely also distinct gene expression mechanisms that differentiate cognitive function and normal age-related brain changes from pathways related to dementia. Individuals who never develop dementia or significant cognitive decline still experience brain deterioration in normal aging, which includes gray and white matter loss and ventricular enlargement that is accompanied by memory decline [93]. Further, previous GWASs for general cognitive function and AD have shown few overlapping loci [21,94]. In addition, studies of older individuals who are cognitively "resilient" with intact cognitive function, despite the presence of AD neuropathology, have found the genetic architecture of cognitive resilience to be distinct from that of AD [95]. As such, relatively little is known about the pathways underlying cognitive aging in those without dementia. Thus, studying gene expression mechanisms that affect general cognitive function before the development of dementia may shed light on cognitive aging without dementia.

Interestingly, while our study's TWASs for AD (EA and AA), WMH, and general cognitive function did not reveal overlapping genes across all four outcomes, we did identify shared underlying metabolic pathways and signaling processes. Specifically, we identified genes related to insulin signaling, whose dysfunction has been implicated in synaptic dysfunction, neuroinflammation, and AD pathologies. Insulin, an anabolic hormone that regulates glucose metabolism, is able to freely cross the blood–brain barrier from the circulatory system and is known to support cognition and enhance the outgrowth of neurons [96]. Studies have shown that insulin resistance, a hallmark of type 2 diabetes, can lead to cognitive decline and is associated with the development of AD [97]. METRO-identified genes for AD (EA and AA), WMH, and general cognitive function have been implicated in insulin resistance and metabolic dysfunction. For instance, for AD, *TOMM40* has been associated with mitochondrial dysfunction and neuroinflammation, which can exacerbate insulin resistance [98], while *APOE*, particularly the *APOE-ε*4 allele, is a well-established risk factor for late-onset AD and has been shown to interfere with insulin receptor signaling, trapping insulin receptors in endosomes and impairing their function [99]. For WMH, *WBP2* has been shown to play a role in the endocrine system, suggesting its involvement in insulin signaling, lipid metabolism, and other metabolic functions [100,101]. Lastly, for general cognitive function, *FOXO6* integrates insulin signaling with gluconeogenesis in

the liver [102,103] and *INS* encodes the peptide hormone insulin, which plays a crucial role in regulating the carbohydrate and lipid metabolisms [104]. Collectively, our findings highlight the complex interplay between insulin signaling, metabolic dysfunction, and cognitive health, underscoring the potential for therapeutic strategies impacting these pathways to mitigate the impacts of cognitive aging and AD.

We also compared genes identified by METRO after fine-mapping with those identified by TWAS-Fusion in Sargurupremraj et al. (2020) [22] and Bellenguez et al. (2022) [23]. Among the 92 genes associated with WMH in Sargurupremraj et al. (2020) [22] and 23 genes identified by METRO, 10 genes overlapped. We note that Sargurupremraj et al. (2020) [22] did not perform the fine-mapping of their TWAS results, which is likely why we identified substantially fewer genes. There were also 10 overlapping genes among the 66 genes associated with AD in Bellenguez et al. (2022) [23] and 69 genes identified by METRO. For both TWAS comparisons, a relatively small number of genes overlapped, likely due to differences in eQTL prediction modeling. Sargurupremraj et al. (2020) [22] and Bellenguez et al. (2022) [23] used eQTL data from brain tissue, while we used eQTL data from transformed beta lymphocytes in blood tissue. While brain tissue is more relevant to WMH and AD phenotypes, blood cells do touch every cell bed that affects the brain and are related to chronic inflammation, immunity, and oxidative stress, which are linked to cognitive performance and dementia. TWAS results from blood tissue from multiple ancestries provide complementary information to those reported in GWASs.

Several limitations in the present study should be noted. First, our gene expression levels were measured using transformed B-lymphocytes from immortalized cell lines in GENOA. While transformed B-lymphocytes are a convenient source of DNA from blood tissue, we lack eQTL data for the tissues that may be most relevant for AD and WMH (e.g., brain tissue, small brain vessels, and microglia). However, B-lymphocytes provide a unique and efficient way to examine the functional effects of genetic variations on gene expression while minimizing environmental influences [105]. Second, METRO follows the standard TWAS approach of analyzing one gene at a time. Since genes residing in the same genomic region may share eQTLs or contain eQTL SNPs that are in LD with each other, the TWAS test statistics of genes in the same region may be highly correlated. To this end, it may be challenging to identify the truly biologically relevant genes among them [25,106]. As such, we paired METRO with FOCUS to allow us to narrow down the list of potential causal genes for AD, VaD, and cognitive decline [25,107]. In addition, we primarily utilized EA GWASs that were publicly available with large sample sizes for general cognitive function, WMH, and AD. As expected, the gene expression prediction models constructed in the same ancestry as the GWAS (EA) tended to have larger contribution weights than those for AA. While we conducted a TWAS of AD in AA individuals, the sample size of the AA GWAS likely did not allow us to properly power our TWAS. As such, a future direction would be to conduct TWASs of these traits using summary statistics from well-powered GWASs with AA ancestry or multiple ancestries as they become available. Lastly, while our study focused on the relationship between genetically regulated expression and neurocognitive outcomes, research has shown that environmental factors, individual lifestyle factors, and epigenetic factors interact with and influence gene expression, which also affects neurocognitive differences [108–130]. For example, to investigate the underlying biological pathways of cognitive aging, recent investigations by our group and others have begun to elucidate the underlying pathways of cognitive aging by examining these complex relationships [108,117,131–134]. Future studies would benefit from the incorporation of information on environmental and individual lifestyle factors, as well as multi-omic data, across ancestry groups to better understand ancestry-specific gene expression differences.

While a full characterization of the genes associated with neurocognitive traits is beyond the scope of this study, previous studies have functionally characterized and experimentally validated some of these identified genes. For instance, studies of postmortem brain tissue from individuals carrying an *APOE-ε4* allele [135,136], as well as investigations using *TREM2* knockout human cell lines [137,138], have shown an earlier onset and more abundant amyloid pathology in such brain tissue. Additionally, genes like *CALCRL* and *EFEMP1* have shown potential neuroprotective effects and associations with neuroinflammation in AD-related conditions [139–142]. Further functional validation of the identified genes in future studies would allow for an enhanced biological interpretation of our findings. The inability to replicate or validate significant genes using additional datasets poses a challenge to the generalizability of our findings. Future studies incorporating larger and more diverse cohorts, as well as integrating multi-omic data, will be crucial for overcoming these limitations and providing a more comprehensive understanding of the genetic factors influencing neurocognitive traits.

Our study also has notable strengths. To the best of our knowledge, our study is the first TWAS using expression mapping studies in multiple ancestries (EA and AA) to identify genes associated with cognitive function and neurocognitive disorders. By conducting a TWAS, we identified putatively causal genes whose expression levels were associated with AD, VaD, and general cognitive function risk through genetically regulated expression, leveraging eQTLs as instrumental variables [20,143–147]. As such, TWASs can be viewed as a form of two-sample two-stage least squares analysis, which are closely related to Mendelian randomization but specifically tailored for gene expression studies [145]. By leveraging the complementary information in gene expression prediction models constructed in EA and AA populations, as well as the uncertainty in SNP prediction weights, we were able to conduct a highly powered TWAS to identify important gene–trait associations and gene expression mechanisms related to the innate immunity, vascular dysfunction, and neuroinflammation underlying AD, VaD, and general cognitive function. Using METRO, we were also able to estimate the ancestry contribution weights for specific genes and identify the extent to which a gene in EA or AA may contribute to the trait. However, it is noteworthy that the larger contributions of the expression prediction models in the same ancestry as the GWAS (primarily EA in this study) may allow for better predictive performance in the same ancestry. The METRO framework provides a higher statistical power for TWASs as compared to ancestry-specific approaches, which we consider to be crucial in GWAS applications to underrepresented populations with small sample sizes. In Li et al. [20], METRO was compared to various alternative methods, including ancestry-specific TWASs, TWAS meta-analysis, and a combination test that aggregates *p*-values from ancestry-specific TWASs. The comparison considered both Bayesian and Frequentist imputation techniques, where the Bayesian sparse linear mixed model (BSLMM) and the elastic net model were used for gene expression prediction. In both simulation studies and real data applications, METRO provided a well-controlled type-I error and was able to leverage information across multiple gene expression studies to achieve a higher statistical power than the compared methods. These key features of METRO make it well-suited for our multi-ancestry TWAS analysis. We also conducted FOCUS fine-mapping to narrow down a list of putatively causal genes among multiple significant genes in a region. Our results suggest that there are similar pathways that contribute to healthy cognitive aging and the progression of dementia, as well as distinct pathways that are unique to each neuropathology. By understanding overlapping and unique genes and the gene expression mechanisms associated with each outcome, we may identify possible targets for the prevention of and/or treatments for cognitive aging and dementia.

4. Materials and Methods

4.1. Sample

The Genetic Epidemiology Network of Arteriopathy (GENOA)

The GENOA study is a community-based longitudinal study aimed at examining the genetic effects of hypertension and related target organ damage [148]. EA (those who self-identified as non-Hispanic white) and AA (those who self-identified as African American) hypertensive sibships were recruited if at least 2 siblings were clinically diagnosed with hypertension before age 60. All other siblings were invited to participate, regardless of their hypertension status. The exclusion criteria included secondary hypertension, alcoholism or drug abuse, pregnancy, insulin-dependent diabetes mellitus, active malignancy, or serum creatinine levels of >2.5 mg/dL. In Phase I (1996–2001), 1854 AA participants (Jackson, MS, USA) and 1583 EA participants (Rochester, MN, USA) were recruited [148]. In Phase II (2000–2004), 1482 AA and 1239 EA participants were successfully followed up, and their potential target organ damage from hypertension was measured. Demographics, medical history, clinical characteristics, information on medication use, and blood samples were collected in each phase. After data cleaning and quality control, a total of 1032 AA and 801 EA samples with genotype and gene expression data were available for analysis. Written informed consent was obtained from all participants, and approval was granted by participating institutional review boards (University of Michigan, University of Mississippi Medical Center, and Mayo Clinic).

4.2. Measures

4.2.1. Genetic Data

AA and EA blood samples were genotyped using the Affymetrix® Genome-Wide Human SNP Array 6.0 (Santa Clara, CA, USA) or the Illumina 1M-Duo 3.0 BeadChip (San Diego, CA, USA). We followed the procedures outlined by Shang et al. [18] for data processing. For each platform, samples and SNPs with a call rate of <95%, samples with a mismatched sex, and duplicate samples were excluded. After removing outliers identified from a genetic principal component analysis, there were 1599 AA and 1464 EA samples with available genotype data. Imputation was performed using the Segmented HAPlotype Estimation & Imputation Tool (SHAPEIT) v.2.r [149] and IMPUTE v.2 [150] using the 1000 Genomes project phase I integrated variant set release (v.3) in NCBI build 37 (hg19) coordinates (released in March 2012). Imputation for each genotyping platform was performed separately and then combined. The final set of genotype data included 30,022,375 and 26,079,446 genetic variants for AA and EA, respectively. After removing genetic variants with an MAF of ≤ 0.01, an imputation quality score (INFO score) of ≤ 0.4 in any platform-based imputation, and indels, a total of 13,793,193 SNPs in AA and 7727,215 SNPs in EA were available for analysis. We used the GENESIS package [151] in R version 4.3.3 [152] to infer the population structure in the analytic sample and the PC-AiR function was used to extract the first five genotype principal components (PCs) by ancestry group, which were subsequently used to adjust for population structure.

4.2.2. Gene Expression Data

Gene expression levels were measured from Epstein–Barr virus (EBV)-transformed B-lymphoblastoid cell lines (LCLs) created from blood samples from a subset of GENOA AA (n = 1233) and EA (n = 919) individuals. The gene expression levels of the AA samples were measured using the Affymetrix Human Transcriptome Array 2.0, while the gene expression levels of the EA samples were measured using Affymetrix Human Exon 1.0 ST Array. We processed the data from the AA and EA samples separately, following the procedures outlined in Shang et al. [18]. Briefly, the Affymetrix Expression Console

was used for quality control, and all array images passed visual inspection. Affymetrix Power Tool software (version 1.4.1) was used to process raw-intensity data [153]. We normalized Affymetrix CEL files using the Robust Multichip Average (RMA) algorithm, including background correction, quantile normalization, $\log_2$-transformation, and probe set summarization [154]. Linearity was also maintained using GC correction (GCCN), signal space transformation (SST), and gain lock (value = 0.75). We used the Brainarray custom CDF [155] version 19 to map the probes to genes, specifically removing probes with non-unique matching cDNA/EST sequences that could be assigned to more than one gene cluster. As a result, the gene expression data processed through the custom CDF are expected to be free of mapability issues; however, alignment bias may still exist due to genetic variation, errors in the reference genome, and other complications [156]. After mapping, Combat was used to remove batch effects [157]. Gene expression data were then quantile-normalized across genes.

4.2.3. GWAS Summary Statistics

We used summary statistics from GWASs for general cognitive function [21], WMH [22], AD in EA [23], and AD in AA [24] as inputs for METRO. Three of the GWASs, Davies et al. (2018) [21], Sargurupremraj et al. (2020) [22], and Bellenguez et al. (2022) [23], were selected because they are the largest meta-analyses to date with publicly available summary statistics; however, we note that all three were conducted primarily with EA samples. We also selected the Kunkle et al. (2021) [24] GWAS because it is the largest meta-analysis to date with public available summary statistics for primarily AA samples. Below, we describe each GWAS and also provide information about the corresponding TWAS analyses that were reported in two of the input GWASs (WMH [22] and AD in EA [23]), which use the same GWAS summary statistics as our analysis but different gene expression data.

General Cognitive Function

We obtained the GWAS summary statistics for general cognitive function from a meta-analysis by Davies et al. (2018) [21], which includes the Cohorts for Heart and Aging Research in Genomic Epidemiology (CHARGE), the Cognitive Genomics Consortium (COGENT) consortia, and the UK Biobank (UKB; Table 1) [21]. This study included 300,486 EA individuals with ages between 16 and 102 years from 57 population-based cohorts. This is the largest available GWAS for general cognitive function, and there are currently no large-scale GWASs available in non-EA populations. General cognitive function was constructed from a number of cognitive tasks. Each cohort was required to have tasks that tested at least three different cognitive domains. PC analysis was performed on the cognitive test scores within each cohort, and the first unrotated component was extracted as the measure of general cognitive function. The models performed within each cohort were adjusted for age, sex, and population stratification. The exclusion criteria included clinical stroke (including self-reported stroke) or prevalent dementia.

White Matter Hyperintensity

We obtained the GWAS summary statistics for WMH from a meta-analysis conducted by Sargurupremraj et al. (2020) that included 48,454 EA and 2516 AA individuals with mean age of 66.0 (SD = 7.5) years from 23 population-based studies from the CHARGE consortium and UKB (Table 1) [22]. We obtained publicly available GWAS summary statistics from only EA individuals. Only summary statistics for EA samples are publicly available for this GWAS. WMH was measured from MRI scans obtained from scanners with field strengths ranging from 1.5 to 3.0 Tesla and interpreted using a standardized protocol blinded to clinical and demographic features. In addition to T1- and T2-weighted scans,

some cohorts included fluid-attenuated inversion recovery (FLAIR) and/or proton density (PD) sequences to measure WMH from cerebrospinal fluid. WMH volume measures were inverse normal transformed, and models were adjusted for sex, age, genetic PCs, and intracranial volume (ICV). The exclusion criteria included a history of stroke or other pathologies that influence the measurement of WMH at the time of MRI.

To functionally characterize and prioritize individual WMH genomic risk loci, Sargurupremraj et al. [22] (2020) conducted a TWAS using TWAS-Fusion [144] with summary statistics from the WMH SNP main effects (EA only) analysis and weights from gene expression reference panels from blood (Netherlands Twin Registry; Young Finns Study), arterial (Genotype-Tissue Expression, GTEx), brain (GTEx, CommonMind Consortium), and peripheral nerve tissue (GTEx). This study did not perform fine-mapping following the TWAS analysis.

Alzheimer's Disease (GWAS in EA)

We obtained the EA GWAS summary statistics for Alzheimer's disease from a stage I meta-analysis by Bellenguez et al. (2022) [23] that included EA samples from the European Alzheimer and Dementia Biobank (EADB), GR@ACE, EADI, GERAD/PERADES, DemGene, Bonn, the Rotterdam study, CCHS study, NxC, and the UKB (Table 1) [23]. The meta-analysis was performed on 39,106 clinically diagnosed AD cases, 46,828 proxy AD and related dementia (ADD) cases, and 401,577 controls. AD cases were clinically diagnosed in all cohorts except UKB, where individuals were identified as proxy ADD cases if their parents had dementia. Participants without a clinical diagnosis of AD, or those without any family history of dementia, were used as controls. Models performed within each cohort were adjusted for PCs and genotyping centers when necessary.

To examine the downstream effects of new AD-associated variants on molecular phenotypes in various AD-relevant tissues, Bellenguez et al. (2022) [23] conducted a TWAS with stage I AD GWAS results. The TWAS was performed by training functional expression and splicing reference panels based on the Accelerating Medicines Partnership (AMP) AD bulk brain and EADB lymphoblastoid cell line (LCL) cohorts, while leveraging precalculated reference panel weights [158] for the GTEx dataset [159] in tissues and cells of interest. TWAS associations were then fine-mapped using Fine-mapping Of CaUsal gene Sets (FOCUS) [25].

Alzheimer's Disease (GWAS in AA)

We also acquired the AA GWAS summary statistics for Alzheimer's disease from a meta-analysis by Kunkle et al. (2021) [24] that included individuals of African American ancestry from 15 cohort studies from the AD Genetics Consortium (ADGC; Table 1). The meta-analysis was performed on 2748 clinically diagnosed AD cases and 5222 controls with a mean age of 74.2 years (SD = 13.6). The models performed within each cohort were adjusted for age, sex, and genetic PCs.

4.3. Statistical Methods

4.3.1. Multi-Ancestry Transcriptome-Wide Association Study

Using the Multi-ancEstry TRanscriptOme-wide (METRO) analysis [20], we conducted a high-powered TWAS with calibrated type I error control to identify the key gene–trait associations and gene expression mechanisms underlying general cognitive function, WMH, and AD. Since gene expression prediction models constructed in different ancestries may contain complementary information, even when the input GWAS was conducted in a single ancestry [20], we used METRO to model gene expressions from EA and AA simultaneously. METRO uses a joint likelihood framework that accounts for SNP effect size heterogeneity and LD differences across ancestries. The framework selectively upweights information

from the ancestry that has a greater certainty in the gene expression prediction model, increasing power and allowing for characterization of the relative contributions of each ancestry to the TWAS results.

METRO is described in Li et al. [20]. Briefly, each gene is examined separately using gene expression data from M different genetic ancestries. $\boldsymbol{Z_m}$ is the n_m-vector of gene expression measurements on n_m individuals in the mth ancestry with $m \in \{1, \ldots, M\}$. For the gene of interest, all *cis*-SNPs (p), which are in potential linkage disequilibrium (LD) with each other, are extracted as predictors for gene expression. $\boldsymbol{G_m}$ is denoted as the $n_m \times p$ genotype matrix for these *cis*-SNPs. Besides the gene expression data, we also use GWAS summary statistics from n individuals for an outcome trait of interest. $\boldsymbol{\gamma}$ is the n-vector of outcome measurements in the GWAS data and $\boldsymbol{G}$ is the corresponding $n \times p$ genotype matrix on the same set of p *cis*-SNPs. The expression vector $\boldsymbol{z_m}$, the outcome vector $\boldsymbol{\gamma}$, and each column of the genotype matrixes are centered and standardized. $\boldsymbol{G_m}$ and $\boldsymbol{G}$ have a mean of zero and variance of one. For each TWAS, we use GWAS summary statistics in the form of marginal z-scores and an SNP–SNP correlation (LD) matrix estimated with genotype data from GENOA that corresponds with the ancestry of the GWAS (EA or AA). The following equations describe the relationships between the SNPs, gene expression, and the outcome:

$$\boldsymbol{z_m} = \boldsymbol{G_m}\boldsymbol{\beta}_{m} + \boldsymbol{\varepsilon}_m, \tag{1}$$

$$\gamma = \alpha(\boldsymbol{G\beta}) + \varepsilon_y, \tag{2}$$

Equation (1) describes the relationship between gene expression and the *cis*-SNP genotypes in the gene expression study in GENOA for the mth ancestry (EA or AA). β_m is a p vector of the *cis*-SNP effects on the gene expression in the mth ancestry and ε_m is an n_m-vector of residual errors, with each element following an independent and normal distribution $N(0, \sigma^2_m)$ with an ancestry-specific variance σ^2_m. Equation (2) describes the relationship between the genetically regulated gene expression (GReX), calculated from estimated SNP prediction weights, and the outcome trait (general cognitive function, WMH, or AD) from the GWAS. There, $G\beta$ denotes an n-vector of the GReX constructed for the GWAS individuals, where $\beta = \Sigma_m w_m \beta_m$ is a p-vector of SNP effects on the gene expression in the GWAS data, where the weights $\Sigma^M_{m=1} w_m = 1$ and $w_m \geq 0$. The alpha value (α) is the effect of the GReX constructed for the GWAS individuals on the outcome trait and ε_y is an n_m-vector of residual errors, with each element following an independent and normal distribution $N(0, \sigma^2_m)$. Both equations, specified based on separate studies, are connected through the predictive SNP effects on the gene expression (β_m and β). A key assumption made is that the SNP effects on the gene expression in the GWAS, β, can be expressed as a weighted summation of the SNP effects on gene expression in the expression studies conducted across ancestries.

We derived the overall GReX effect α and the contribution weight of each ancestry (w_1 for AA and w_2 for EA) to infer the extent and contribution of the two genetic ancestries in informing the GreX–trait association. The joint model defined in Equations (1) and (2) allows us to borrow association strengths across multiple ancestries to enable powerful inferences of GreX–trait associations for general cognitive function, WMH, and AD. We declared the gene to be significant if the p-value was below the corresponding Bonferroni-corrected threshold for the number of tested genes ($p < 0.05/17,238 = 2.90 \times 10^{-6}$). Manhattan plots and quantile–quantile (Q-Q) plots were generated using the *qqman* [160] R package.

4.3.2. Fine-Mapping Analysis

Since genes residing in the same genomic region may share eQTLs or contain eQTL SNPs in LD with each other, TWAS test statistics for genes in the same region can be

highly correlated, making it difficult to identify the true biologically relevant genes among them. To prioritize the putatively causal genes identified by METRO for general cognitive function, WMH, and AD, we conducted TWAS fine-mapping using FOCUS (Fine-mapping Of CaUsal gene Sets) [25]. To identify a genomic region with at least one significant gene detected by METRO, we obtained a set of independent, non-overlapping genomic regions, or LD blocks, using Ldetect [161]. In each analyzed genomic block, using a standard Bayesian approach, we assigned a posterior inclusion probability (PIP) for each gene to be causal, given the observed TWAS statistics. We used gene-level Z scores, created from *p*-values using the inverse cumulative distribution function (CDF) of a standard normal distribution, as inputs for FOCUS. We then ranked the PIPs and computed the 90%-credible set that contained the causal gene with a 90% probability. In the FOCUS analysis, a null model which assumed none of the genes in the region were causally associated with the trait was also considered as a possible outcome and may be included in the credible set. Through fine-mapping, we narrowed down significantly associated genes identified by METRO to a shorter list of putatively true associations.

4.3.3. Characterization of Identified Genes

To interpret our TWAS findings, both before and after fine-mapping, we further examined whether the genes identified by METRO overlapped with those previously identified by their corresponding input GWASs. We created a set of Venn diagrams of overlapping genes identified using METRO with those from the SNP-based GWAS association results [21–24] mapped to the nearest gene using the *VennDiagram* R package [162]. We then constructed a second set of Venn diagrams showing the overlapping genes identified using METRO with genes identified by gene-based association analyses in each of the input GWASs. The gene-based analyses were conducted using MAGMA [163] (general cognitive function [21], WMH [22], and AD (AA GWAS) [24]) or gene prioritization tests (AD (EA GWAS) [23]). Finally, we created a set of Venn diagrams comparing the genes identified using METRO with those identified in the TWASs that were conducted as part of the WMH [22] and AD (EA GWAS) [23] input GWASs. We used the *geneSynonym* R package [164] to ensure that genes named differently across studies were captured.

4.3.4. Functional Enrichment Analysis

To characterize the biological function of the genes identified by METRO for general cognitive function, WMH, and AD, we performed gene set enrichment analysis. Specifically, we used the g:GOSt [165] tool on the web software g:Profiler (version e112_eg59_p19_25aa4782) and mapped the genes to known functional informational sources, including Gene Ontology (GO): molecular function (MF), GO: biological process (BP), GO: cellular component (CC), Kyoto Encyclopedia of Genes and Genomes (KEGG), Reactome (REAC), WikiPathways (WP), Transfac (TF), MiRTarBase (MIRNA), Human Protein Atlas (HPA), CORUM protein complexes, and Human Phenotype Ontology (HP). In this analysis, we used the default option g:SCS method (Set Counts and Sizes) in g:Profiler for multiple testing correction and presented the pathways identified with an adjusted *p*-value < 0.05. Driver terms in GO are highlighted using a two-stage algorithm for filtering GO enrichment results, providing a more efficient and reliable approach compared to traditional clustering methods. This feature groups significant terms into sub-ontologies based on their relations, and the second stage identifies leading gene sets that give rise to other significant functions in the same group of terms. This method uses a greedy search strategy that recalculates hypergeometric *p*-values and results in the consideration of multiple leading terms in a component, rather than selection of terms with the highest significance level.

5. Conclusions

In the present study, we conducted a multi-ancestry TWAS in EA and AA populations to identify genes associated with general cognitive function, WMH, and AD. We identified genes associated with innate immunity, vascular dysfunction, and neuroinflammation. The WMH and AD TWASs also indicated that the downregulation of *ICA1L* may contribute to overlapping AD and VaD neuropathology. To our knowledge, this study is the first TWAS analysis using expression mapping studies in multiple ancestries to increase the power to identify genes associated with cognitive function and neurocognitive disorders, which may help to identify gene targets for pharmaceutical or preventative treatment for dementia.

References

1. 2023 Alzheimer's Disease Facts and Figures. *Alzheimer's Dement.* **2023**, *19*, 1598–1695. [CrossRef] [PubMed]
2. De Reuck, J.; Maurage, C.-A.; Deramecourt, V.; Pasquier, F.; Cordonnier, C.; Leys, D.; Bordet, R. Aging and Cerebrovascular Lesions in Pure and in Mixed Neurodegenerative and Vascular Dementia Brains: A Neuropathological Study. *Folia Neuropathol.* **2018**, *56*, 81–87. [CrossRef]
3. Hof, P.R.; Glannakopoulos, P.; Bouras, C. The Neuropathological Changes Associated with Normal Brain Aging. *Histol. Histopathol.* **1996**, *11*, 1075–1088. [PubMed]
4. Perl, D.P. Neuropathology of Alzheimer's Disease. *Mt. Sinai J. Med.* **2010**, *77*, 32–42. [CrossRef] [PubMed]
5. Cohuet, G.; Struijker-Boudier, H. Mechanisms of Target Organ Damage Caused by Hypertension: Therapeutic Potential. *Pharmacol. Ther.* **2006**, *111*, 81–98. [CrossRef]
6. Weller, J.; Budson, A. Current Understanding of Alzheimer's Disease Diagnosis and Treatment. *F1000Research* **2018**, *7*, F1000 Faculty Rev-1161. [CrossRef]

7. Hubbard, B.M.; Fenton, G.W.; Anderson, J.M. A Quantitative Histological Study of Early Clinical and Preclinical Alzheimer's Disease. *Neuropathol. Appl. Neurobiol.* **1990**, *16*, 111–121. [CrossRef]

8. Sperling, R.A.; Aisen, P.S.; Beckett, L.A.; Bennett, D.A.; Craft, S.; Fagan, A.M.; Iwatsubo, T.; Jack, C.R.; Kaye, J.; Montine, T.J.; et al. Toward Defining the Preclinical Stages of Alzheimer's Disease: Recommendations from the National Institute on Aging-Alzheimer's Association Workgroups on Diagnostic Guidelines for Alzheimer's Disease. *Alzheimer's Dement.* **2011**, *7*, 280–292. [CrossRef]

9. Mayeda, E.R.; Glymour, M.M.; Quesenberry, C.P.; Whitmer, R.A. Inequalities in Dementia Incidence between Six Racial and Ethnic Groups over 14 Years. *Alzheimer's Dement.* **2016**, *12*, 216–224. [CrossRef]

10. Barnes, L.L.; Bennett, D.A. Alzheimer's Disease in African Americans: Risk Factors and Challenges for the Future. *Health Aff.* **2014**, *33*, 580–586. [CrossRef]

11. Brewster, P.; Barnes, L.; Haan, M.; Johnson, J.K.; Manly, J.J.; Nápoles, A.M.; Whitmer, R.A.; Carvajal-Carmona, L.; Early, D.; Farias, S.; et al. Progress and Future Challenges in Aging and Diversity Research in the United States. *Alzheimer's Dement.* **2019**, *15*, 995–1003. [CrossRef] [PubMed]

12. Rajan, K.B.; Weuve, J.; Barnes, L.L.; Wilson, R.S.; Evans, D.A. Prevalence and Incidence of Clinically Diagnosed Alzheimer's Disease Dementia from 1994 to 2012 in a Population Study. *Alzheimer's Dement.* **2019**, *15*, 1–7. [CrossRef] [PubMed]

13. Cacabelos, R.; Torrellas, C. Epigenetics of Aging and Alzheimer's Disease: Implications for Pharmacogenomics and Drug Response. *Int. J. Mol. Sci.* **2015**, *16*, 30483–30543. [CrossRef] [PubMed]

14. Tam, V.; Patel, N.; Turcotte, M.; Bossé, Y.; Paré, G.; Meyre, D. Benefits and Limitations of Genome-Wide Association Studies. *Nat. Rev. Genet.* **2019**, *20*, 467–484. [CrossRef]

15. Lappalainen, T.; Sammeth, M.; Friedländer, M.R.; 't Hoen, P.A.; Monlong, J.; Rivas, M.A.; Gonzàlez-Porta, M.; Kurbatova, N.; Griebel, T.; Ferreira, P.G.; et al. Transcriptome and Genome Sequencing Uncovers Functional Variation in Humans. *Nature* **2013**, *501*, 506–511. [CrossRef]

16. Mogil, L.S.; Andaleon, A.; Badalamenti, A.; Dickinson, S.P.; Guo, X.; Rotter, J.I.; Johnson, W.C.; Im, H.K.; Liu, Y.; Wheeler, H.E. Genetic Architecture of Gene Expression Traits across Diverse Populations. *PLoS Genet.* **2018**, *14*, e1007586. [CrossRef]

17. Wojcik, G.; Graff, M.; Nishimura, K.; Tao, R.; Haessler, J.; Gignoux, C.; Highland, H.; Patel, Y.; Sorokin, E.; Avery, C.; et al. Genetic Analyses of Diverse Populations Improves Discovery for Complex Traits. *Nature* **2019**, *570*, 514–518. [CrossRef]

18. Shang, L.; Smith, J.A.; Zhao, W.; Kho, M.; Turner, S.T.; Mosley, T.H.; Kardia, S.L.R.; Zhou, X. Genetic Architecture of Gene Expression in European and African Americans: An eQTL Mapping Study in GENOA. *Am. J. Hum. Genet.* **2020**, *106*, 496–512. [CrossRef]

19. Nica, A.C.; Dermitzakis, E.T. Expression Quantitative Trait Loci: Present and Future. *Philos. Trans. R. Soc. Lond. B Biol. Sci.* **2013**, *368*, 20120362. [CrossRef]

20. Li, Z.; Zhao, W.; Shang, L.; Mosley, T.H.; Kardia, S.L.R.; Smith, J.A.; Zhou, X. METRO: Multi-Ancestry Transcriptome-Wide Association Studies for Powerful Gene-Trait Association Detection. *Am. J. Hum. Genet.* **2022**, *109*, 783–801. [CrossRef]

21. Davies, G.; Lam, M.; Harris, S.E.; Trampush, J.W.; Luciano, M.; Hill, W.D.; Hagenaars, S.P.; Ritchie, S.J.; Marioni, R.E.; Fawns-Ritchie, C.; et al. Study of 300,486 Individuals Identifies 148 Independent Genetic Loci Influencing General Cognitive Function. *Nat. Commun.* **2018**, *9*, 2098. [CrossRef] [PubMed]

22. Sargurupremraj, M.; Suzuki, H.; Jian, X.; Sarnowski, C.; Evans, T.E.; Bis, J.C.; Eiriksdottir, G.; Sakaue, S.; Terzikhan, N.; Habes, M.; et al. Cerebral Small Vessel Disease Genomics and Its Implications across the Lifespan. *Nat. Commun.* **2020**, *11*, 6285. [CrossRef]

23. Bellenguez, C.; Küçükali, F.; Jansen, I.E.; Kleineidam, L.; Moreno-Grau, S.; Amin, N.; Naj, A.C.; Campos-Martin, R.; Grenier-Boley, B.; Andrade, V.; et al. New Insights into the Genetic Etiology of Alzheimer's Disease and Related Dementias. *Nat. Genet.* **2022**, *54*, 412–436. [CrossRef] [PubMed]

24. Kunkle, B.W.; Schmidt, M.; Klein, H.-U.; Naj, A.C.; Hamilton-Nelson, K.L.; Larson, E.B.; Evans, D.A.; De Jager, P.L.; Crane, P.K.; Buxbaum, J.D.; et al. Novel Alzheimer Disease Risk Loci and Pathways in African American Individuals Using the African Genome Resources Panel: A Meta-Analysis. *JAMA Neurol.* **2021**, *78*, 102–113. [CrossRef] [PubMed]

25. Mancuso, N.; Freund, M.K.; Johnson, R.; Shi, H.; Kichaev, G.; Gusev, A.; Pasaniuc, B. Probabilistic Fine-Mapping of Transcriptome-Wide Association Studies. *Nat. Genet.* **2019**, *51*, 675–682. [CrossRef]

26. Chagnot, A.; Barnes, S.R.; Montagne, A. Magnetic Resonance Imaging of Blood–Brain Barrier Permeability in Dementia. *Neuroscience* **2021**, *474*, 14–29. [CrossRef]

27. Kalaria, R.N.; Sepulveda-Falla, D. Cerebral Small Vessel Disease in Sporadic and Familial Alzheimer Disease. *Am. J. Pathol.* **2021**, *191*, 1888–1905. [CrossRef]

28. Zhang, C.; Qin, F.; Li, X.; Du, X.; Li, T. Identification of Novel Proteins for Lacunar Stroke by Integrating Genome-Wide Association Data and Human Brain Proteomes. *BMC Med.* **2022**, *20*, 211. [CrossRef]

29. Bai, B.; Vanderwall, D.; Li, Y.; Wang, X.; Poudel, S.; Wang, H.; Dey, K.K.; Chen, P.-C.; Yang, K.; Peng, J. Proteomic Landscape of Alzheimer's Disease: Novel Insights into Pathogenesis and Biomarker Discovery. *Mol. Neurodegener.* **2021**, *16*, 55. [CrossRef]

30. Wingo, A.P.; Liu, Y.; Gerasimov, E.S.; Gockley, J.; Logsdon, B.A.; Duong, D.M.; Dammer, E.B.; Robins, C.; Beach, T.G.; Reiman, E.M.; et al. Integrating Human Brain Proteomes with Genome-Wide Association Data Implicates New Proteins in Alzheimer's Disease Pathogenesis. *Nat. Genet.* **2021**, *53*, 143–146. [CrossRef]

31. Ou, Y.-N.; Yang, Y.-X.; Deng, Y.-T.; Zhang, C.; Hu, H.; Wu, B.-S.; Liu, Y.; Wang, Y.-J.; Zhu, Y.; Suckling, J.; et al. Identification of Novel Drug Targets for Alzheimer's Disease by Integrating Genetics and Proteomes from Brain and Blood. *Mol. Psychiatry* **2021**, *26*, 6065–6073. [CrossRef] [PubMed]

32. Cullell, N.; Gallego-Fábrega, C.; Cárcel-Márquez, J.; Muiño, E.; Llucià-Carol, L.; Lledós, M.; Martín-Campos, J.M.; Molina, J.; Casas, L.; Almeria, M.; et al. ICA1L Is Associated with Small Vessel Disease: A Proteome-Wide Association Study in Small Vessel Stroke and Intracerebral Haemorrhage. *Int. J. Mol. Sci.* **2022**, *23*, 3161. [CrossRef] [PubMed]

33. Liu, D.-Z.; Sharp, F.R. Excitatory and Mitogenic Signaling in Cell Death, Blood–Brain Barrier Breakdown, and BBB Repair after Intracerebral Hemorrhage. *Transl. Stroke Res.* **2012**, *3*, 62–69. [CrossRef] [PubMed]

34. Lai, T.W.; Zhang, S.; Wang, Y.T. Excitotoxicity and Stroke: Identifying Novel Targets for Neuroprotection. *Prog. Neurobiol.* **2014**, *115*, 157–188. [CrossRef]

35. Ge, Y.-J.; Ou, Y.-N.; Deng, Y.-T.; Wu, B.-S.; Yang, L.; Zhang, Y.-R.; Chen, S.-D.; Huang, Y.-Y.; Dong, Q.; Tan, L.; et al. Prioritization of Drug Targets for Neurodegenerative Diseases by Integrating Genetic and Proteomic Data From Brain and Blood. *Biol. Psychiatry* **2023**, *93*, 770–779. [CrossRef]

36. Uchida, Y.; Kan, H.; Furukawa, G.; Onda, K.; Sakurai, K.; Takada, K.; Matsukawa, N.; Oishi, K. Relationship between Brain Iron Dynamics and Blood-Brain Barrier Function during Childhood: A Quantitative Magnetic Resonance Imaging Study. *Fluids Barriers CNS* **2023**, *20*, 60. [CrossRef]

37. Uchida, Y.; Kan, H.; Sakurai, K.; Oishi, K.; Matsukawa, N. Contributions of Blood-Brain Barrier Imaging to Neurovascular Unit Pathophysiology of Alzheimer's Disease and Related Dementias. *Front. Aging Neurosci.* **2023**, *15*, 1111448. [CrossRef]

38. Yamanaka, T.; Uchida, Y.; Sakurai, K.; Kato, D.; Mizuno, M.; Sato, T.; Madokoro, Y.; Kondo, Y.; Suzuki, A.; Ueki, Y.; et al. Anatomical Links between White Matter Hyperintensity and Medial Temporal Atrophy Reveal Impairment of Executive Functions. *Aging Dis.* **2019**, *10*, 711–718. [CrossRef]

39. Uchida, Y.; Kan, H.; Sakurai, K.; Horimoto, Y.; Hayashi, E.; Iida, A.; Okamura, N.; Oishi, K.; Matsukawa, N. APOE ε4 Dose Associates with Increased Brain Iron and β-Amyloid via Blood-Brain Barrier Dysfunction. *J. Neurol. Neurosurg. Psychiatry* **2022**, *93*, 772–778. [CrossRef]

40. Kanehisa, M.; Furumichi, M.; Sato, Y.; Ishiguro-Watanabe, M.; Tanabe, M. KEGG: Integrating Viruses and Cellular Organisms. *Nucleic Acids Res.* **2021**, *49*, D545–D551. [CrossRef]

41. De Bruijn, M.F.; Speck, N.A. Core-Binding Factors in Hematopoiesis and Immune Function. *Oncogene* **2004**, *23*, 4238–4248. [CrossRef] [PubMed]

42. Maillard, I.; Adler, S.H.; Pear, W.S. Notch and the Immune System. *Immunity* **2003**, *19*, 781–791. [CrossRef] [PubMed]

43. Radtke, F.; Wilson, A.; Mancini, S.J.C.; MacDonald, H.R. Notch Regulation of Lymphocyte Development and Function. *Nat. Immunol.* **2004**, *5*, 247–253. [CrossRef] [PubMed]

44. Rothenberg, E.V.; Taghon, T. Molecular Genetics of T Cell Development. *Annu. Rev. Immunol.* **2005**, *23*, 601–649. [CrossRef] [PubMed]

45. Shapiro-Shelef, M.; Calame, K. Regulation of Plasma-Cell Development. *Nat. Rev. Immunol.* **2005**, *5*, 230–242. [CrossRef]

46. Spits, H. Development of Aβ T Cells in the Human Thymus. *Nat. Rev. Immunol.* **2002**, *2*, 760–772. [CrossRef]

47. Lambert, J.-C.; Ibrahim-Verbaas, C.A.; Harold, D.; Naj, A.C.; Sims, R.; Bellenguez, C.; Jun, G.; DeStefano, A.L.; Bis, J.C.; Beecham, G.W.; et al. Meta-Analysis of 74,046 Individuals Identifies 11 New Susceptibility Loci for Alzheimer's Disease. *Nat. Genet.* **2013**, *45*, 1452–1458. [CrossRef]

48. Hollingworth, P.; Harold, D.; Sims, R.; Gerrish, A.; Lambert, J.-C.; Carrasquillo, M.M.; Abraham, R.; Hamshere, M.L.; Pahwa, J.S.; Moskvina, V.; et al. Common Variants in ABCA7, MS4A6A/MS4A4E, EPHA1, CD33 and CD2AP Are Associated with Alzheimer's Disease. *Nat. Genet.* **2011**, *43*, 429–435. [CrossRef]

49. Reitz, C.; Mayeux, R. Genetics of Alzheimer's Disease in Caribbean Hispanic and African American Populations. *Biol. Psychiatry* **2014**, *75*, 534–541. [CrossRef]

50. Reitz, C.; Jun, G.; Naj, A.; Rajbhandary, R. Variants in the ATP-Binding Cassette Transporter (ABCA7), Apolipoprotein E ε4, and the Risk of Late-Onset Alzheimer Disease in African Americans. *JAMA* **2013**, *309*, 1483–1492. [CrossRef]

51. De Roeck, A.; Van Broeckhoven, C.; Sleegers, K. The Role of ABCA7 in Alzheimer's Disease: Evidence from Genomics, Transcriptomics and Methylomics. *Acta Neuropathol.* **2019**, *138*, 201–220. [CrossRef] [PubMed]

52. Guardiola, M.; Muntané, G.; Martínez, I.; Martorell, L.; Girona, J.; Ibarretxe, D.; Plana, N.; Bullido, M.J.; Vilella, E.; Ribalta, J. Metabolic Overlap between Alzheimer's Disease and Metabolic Syndrome Identifies the PVRL2 Gene as a New Modulator of Diabetic Dyslipidemia. *Int. J. Mol. Sci.* **2023**, *24*, 7415. [CrossRef] [PubMed]

53. Liang, X.; Liu, C.; Liu, K.; Cong, L.; Wang, Y.; Liu, R.; Fa, W.; Tian, N.; Cheng, Y.; Wang, N.; et al. Association and Interaction of TOMM40 and PVRL2 with Plasma Amyloid-β and Alzheimer's Disease among Chinese Older Adults: A Population-Based Study. *Neurobiol. Aging* **2022**, *113*, 143–151. [CrossRef] [PubMed]

54. Chatterjee, P.; Roy, D.; Bhattacharyya, M.; Bandyopadhyay, S. Biological Networks in Parkinson's Disease: An Insight into the Epigenetic Mechanisms Associated with This Disease. *BMC Genom.* **2017**, *18*, 721. [CrossRef]

55. Gialluisi, A.; Reccia, M.G.; Modugno, N.; Nutile, T.; Lombardi, A.; Di Giovannantonio, L.G.; Pietracupa, S.; Ruggiero, D.; Scala, S.; Gambardella, S.; et al. Identification of Sixteen Novel Candidate Genes for Late Onset Parkinson's Disease. *Mol. Neurodegener.* **2021**, *16*, 35. [CrossRef]

56. Salem, M.; Ammitzboell, M.; Nys, K.; Seidelin, J.B.; Nielsen, O.H. ATG16L1: A Multifunctional Susceptibility Factor in Crohn Disease. *Autophagy* **2015**, *11*, 585–594. [CrossRef]

57. Hansson, O.; Kumar, A.; Janelidze, S.; Stomrud, E.; Insel, P.S.; Blennow, K.; Zetterberg, H.; Fauman, E.; Hedman, Å.K.; Nagle, M.W.; et al. The Genetic Regulation of Protein Expression in Cerebrospinal Fluid. *EMBO Mol. Med.* **2023**, *15*, e16359. [CrossRef]

58. Cali, E.; Dominik, N.; Manole, A.; Houlden, H. Riboflavin Transporter Deficiency. In *GeneReviews®*; Adam, M.P., Mirzaa, G.M., Pagon, R.A., Wallace, S.E., Bean, L.J., Gripp, K.W., Amemiya, A., Eds.; University of Washington, Seattle: Seattle, WA, USA, 1993.

59. Novikova, G.; Kapoor, M.; Tcw, J.; Abud, E.M.; Efthymiou, A.G.; Chen, S.X.; Cheng, H.; Fullard, J.F.; Bendl, J.; Liu, Y.; et al. Integration of Alzheimer's Disease Genetics and Myeloid Genomics Identifies Disease Risk Regulatory Elements and Genes. *Nat. Commun.* **2021**, *12*, 1610. [CrossRef]

60. Allan, C.M.; Walker, D.; Segrest, J.P.; Taylor, J.M. Identification and Characterization of a New Human Gene (APOC4) in the Apolipoprotein E, C-I, and C-II Gene Locus. *Genomics* **1995**, *28*, 291–300. [CrossRef]

61. Wang, P.; Luo, M.; Zhou, W.; Jin, X.; Xu, Z.; Yan, S.; Li, Y.; Xu, C.; Cheng, R.; Huang, Y.; et al. Global Characterization of Peripheral B Cells in Parkinson's Disease by Single-Cell RNA and BCR Sequencing. *Front. Immunol.* **2022**, *13*, 814239. [CrossRef]

62. Yu, L.P.; Sheehy, M.J. The Cryptic HLA-DQA2 ("DX Alpha") Gene Is Expressed in Human B Cell Lines. *J. Immunol.* **1991**, *147*, 4393–4397. [CrossRef] [PubMed]

63. Li, G.-J.; Yang, Q.-H.; Yang, G.-K.; Yang, G.; Hou, Y.; Hou, L.-J.; Li, Z.-X.; Du, L.-J. MiR-125b and SATB1-AS1 Might Be Shear Stress-Mediated Therapeutic Targets. *Gene* **2023**, *857*, 147181. [CrossRef] [PubMed]

64. Naguib, A.; Sandmann, T.; Yi, F.; Watts, R.J.; Lewcock, J.W.; Dowdle, W.E. SUPT4H1 Depletion Leads to a Global Reduction in RNA. *Cell Rep.* **2019**, *26*, 45–53.e4. [CrossRef]

65. Greaves, C.V.; Rohrer, J.D. An Update on Genetic Frontotemporal Dementia. *J. Neurol.* **2019**, *266*, 2075–2086. [CrossRef] [PubMed]

66. Ballasch, I.; García-García, E.; Vila, C.; Pérez-González, A.; Sancho-Balsells, A.; Fernández, J.; Soto, D.; Puigdellívol, M.; Gasull, X.; Alberch, J.; et al. Ikzf1 as a Novel Regulator of Microglial Homeostasis in Inflammation and Neurodegeneration. *Brain Behav. Immun.* **2023**, *109*, 144–161. [CrossRef]

67. Schutte, B.; Henfling, M.; Ramaekers, F.C.S. DEDD Association with Cytokeratin Filaments Correlates with Sensitivity to Apoptosis. *Apoptosis* **2006**, *11*, 1561–1572. [CrossRef]

68. Dahal, A.; Hinton, S.D. Antagonistic Roles for STYX Pseudophosphatases in Neurite Outgrowth. *Biochem. Soc. Trans.* **2017**, *45*, 381–387. [CrossRef]

69. Burgaletto, C.; Munafò, A.; Di Benedetto, G.; De Francisci, C.; Caraci, F.; Di Mauro, R.; Bucolo, C.; Bernardini, R.; Cantarella, G. The Immune System on the TRAIL of Alzheimer's Disease. *J. Neuroinflamm.* **2020**, *17*, 298. [CrossRef]

70. Traylor, M.; Persyn, E.; Tomppo, L.; Klasson, S.; Abedi, V.; Bakker, M.K.; Torres, N.; Li, L.; Bell, S.; Rutten-Jacobs, L.; et al. Genetic Basis of Lacunar Stroke: A Pooled Analysis of Individual Patient Data and Genome-Wide Association Studies. *Lancet Neurol.* **2021**, *20*, 351–361. [CrossRef]

71. Chen, K.; Zhu, L.; Guo, L.; Pan, Y.-B.; Feng, D.-F. Maf1 Regulates Dendritic Morphogenesis and Influences Learning and Memory. *Cell Death Dis.* **2020**, *11*, 606. [CrossRef]

72. Kumar, A.A.; Yeo, N.; Whittaker, M.; Attra, P.; Barrick, T.R.; Bridges, L.R.; Dickson, D.W.; Esiri, M.M.; Farris, C.W.; Graham, D.; et al. Vascular Collagen Type-IV in Hypertension and Cerebral Small Vessel Disease. *Stroke* **2022**, *53*, 3696–3705. [CrossRef] [PubMed]

73. Miners, S.; van Helmond, Z.; Barker, R.; Passmore, P.A.; Johnston, J.A.; Todd, S.; McGuinness, B.M.; Panza, F.; Seripa, D.; Solfrizzi, V.; et al. Genetic Variation in MME in Relation to Neprilysin Protein and Enzyme Activity, Aβ Levels, and Alzheimer's Disease Risk. *Int. J. Mol. Epidemiol. Genet.* **2012**, *3*, 30–38.

74. Chen, G.; Li, L.; Tao, H. Bioinformatics Identification of Ferroptosis-Related Biomarkers and Therapeutic Compounds in Ischemic Stroke. *Front. Neurol.* **2021**, *12*, 745240. [CrossRef] [PubMed]

75. Pan, Y.; Fu, Y.; Baird, P.N.; Guymer, R.H.; Das, T.; Iwata, T. Exploring the Contribution of ARMS2 and HTRA1 Genetic Risk Factors in Age-Related Macular Degeneration. *Prog. Retin. Eye Res.* **2022**, *97*, 101159. [CrossRef] [PubMed]

76. Thee, E.F.; Colijn, J.M.; Cougnard-Grégoire, A.; Meester-Smoor, M.A.; Verzijden, T.; Hoyng, C.B.; Fauser, S.; Hense, H.-W.; Silva, R.; Creuzot-Garcher, C.; et al. The Phenotypic Course of Age-Related Macular Degeneration for ARMS2/HTRA1: The EYE-RISK Consortium. *Ophthalmology* **2022**, *129*, 752–764. [CrossRef]

77. Gatta, L.B.; Vitali, M.; Zanola, A.; Venturelli, E.; Fenoglio, C.; Galimberti, D.; Scarpini, E.; Finazzi, D. Polymorphisms in the LOC387715/ARMS2 Putative Gene and the Risk for Alzheimer's Disease. *Dement. Geriatr. Cogn. Disord.* **2008**, *26*, 169–174. [CrossRef]

78. Wang, P.; Qin, W.; Wang, P.; Huang, Y.; Liu, Y.; Zhang, R.; Li, S.; Yang, Q.; Wang, X.; Chen, F.; et al. Genomic Variants in NEURL, GJA1 and CUX2 Significantly Increase Genetic Susceptibility to Atrial Fibrillation. *Sci. Rep.* **2018**, *8*, 3297. [CrossRef]

79. Li, R.-G.; Xu, Y.-J.; Ye, W.G.; Li, Y.-J.; Chen, H.; Qiu, X.-B.; Yang, Y.-Q.; Bai, D. Connexin45 (GJC1) Loss-of-Function Mutation Contributes to Familial Atrial Fibrillation and Conduction Disease. *Heart Rhythm.* **2021**, *18*, 684–693. [CrossRef]

80. Zhu, C.; Xiao, F.; Lin, W. EFTUD2 on Innate Immunity. *Oncotarget* **2015**, *6*, 32313–32314. [CrossRef]

81. Abo Elwafa, R.; Gamaleldin, M.; Ghallab, O. The Clinical and Prognostic Significance of FIS1, SPI1, PDCD7 and Ang2 Expression Levels in Acute Myeloid Leukemia. *Cancer Genet.* **2019**, *233–234*, 84–95. [CrossRef]

82. Vadhvani, M.; Schwedhelm-Domeyer, N.; Mukherjee, C.; Stegmüller, J. The Centrosomal E3 Ubiquitin Ligase FBXO31-SCF Regulates Neuronal Morphogenesis and Migration. *PLoS ONE* **2013**, *8*, e57530. [CrossRef] [PubMed]

83. Serpeloni, F.; Nätt, D.; de Assis, S.G.; Wieling, E.; Elbert, T. Experiencing Community and Domestic Violence Is Associated with Epigenetic Changes in DNA Methylation of BDNF and CLPX in Adolescents. *Psychophysiology* **2020**, *57*, e13382. [CrossRef] [PubMed]

84. ZSCAN29 Zinc Finger and SCAN Domain Containing 29 [Homo Sapiens (Human)]—Gene—NCBI. Available online: https://www.ncbi.nlm.nih.gov/gene/146050#summary (accessed on 1 August 2023).

85. Baker, T.A.; Sauer, R.T. ClpXP, an ATP-Powered Unfolding and Protein-Degradation Machine. *Biochim. Et Biophys. Acta (BBA) Mol. Cell Res.* **2012**, *1823*, 15–28. [CrossRef] [PubMed]

86. Thomas, T.; Perdue, M.V.; Khalaf, S.; Landi, N.; Hoeft, F.; Pugh, K.; Grigorenko, E.L. Neuroimaging Genetic Associations between SEMA6D, Brain Structure, and Reading Skills. *J. Clin. Exp. Neuropsychol.* **2021**, *43*, 276–289. [CrossRef]

87. Perdue, M.V.; Mascheretti, S.; Kornilov, S.A.; Jasińska, K.K.; Ryherd, K.; Einar Mencl, W.; Frost, S.J.; Grigorenko, E.L.; Pugh, K.R.; Landi, N. Common Variation within the SETBP1 Gene Is Associated with Reading-Related Skills and Patterns of Functional Neural Activation. *Neuropsychologia* **2019**, *130*, 44–51. [CrossRef]

88. Ziegler, G.C.; Ehlis, A.-C.; Weber, H.; Vitale, M.R.; Zöller, J.E.M.; Ku, H.-P.; Schiele, M.A.; Kürbitz, L.I.; Romanos, M.; Pauli, P.; et al. A Common CDH13 Variant Is Associated with Low Agreeableness and Neural Responses to Working Memory Tasks in ADHD. *Genes* **2021**, *12*, 1356. [CrossRef]

89. Trubetskoy, V.; Pardiñas, A.F.; Qi, T.; Panagiotaropoulou, G.; Awasthi, S.; Bigdeli, T.B.; Bryois, J.; Chen, C.-Y.; Dennison, C.A.; Hall, L.S.; et al. Mapping Genomic Loci Implicates Genes and Synaptic Biology in Schizophrenia. *Nature* **2022**, *604*, 502–508. [CrossRef]

90. Beeri, M.S.; Lin, H.-M.; Sano, M.; Ravona-Springer, R.; Liu, X.; Bendlin, B.B.; Gleason, C.E.; Guerrero-Berroa, E.; Soleimani, L.; Launer, L.J.; et al. Association of the Haptoglobin Gene Polymorphism with Cognitive Function and Decline in Elderly African American Adults with Type 2 Diabetes: Findings From the Action to Control Cardiovascular Risk in Diabetes-Memory in Diabetes (ACCORD-MIND) Study. *JAMA Netw. Open* **2018**, *1*, e184458. [CrossRef]

91. Kikuchi, M.; Yamada, K.; Toyota, T.; Yoshikawa, T. C18orf1 Located on Chromosome 18p11.2 May Confer Susceptibility to Schizophrenia. *J. Med. Dent. Sci.* **2003**, *50*, 225–229.

92. Zhang, Z.; Shang, J.; Dai, Z.; Yao, Y.; Shi, Y.; Zhong, D.; Liang, Y.; Lai, C.; Yang, Q.; Feng, T.; et al. Transmembrane Protein 170B Is a Prognostic Biomarker and Associated With Immune Infiltrates in Pancreatic Adenocarcinoma. *Front. Genet.* **2022**, *13*, 848391. [CrossRef]

93. Ge, Y.; Grossman, R.I.; Babb, J.S.; Rabin, M.L.; Mannon, L.J.; Kolson, D.L. Age-Related Total Gray Matter and White Matter Changes in Normal Adult Brain. Part I: Volumetric MR Imaging Analysis. *Am. J. Neuroradiol.* **2002**, *23*, 1327–1333. [PubMed]

94. Davies, G.; Armstrong, N.; Bis, J.C.; Bressler, J.; Chouraki, V.; Giddaluru, S.; Hofer, E.; Ibrahim-Verbaas, C.A.; Kirin, M.; Lahti, J.; et al. Genetic Contributions to Variation in General Cognitive Function: A Meta-Analysis of Genome-Wide Association Studies in the CHARGE Consortium (N = 53,949). *Mol. Psychiatry* **2015**, *20*, 183–192. [CrossRef] [PubMed]

95. Dumitrescu, L.; Mahoney, E.R.; Mukherjee, S.; Lee, M.L.; Bush, W.S.; Engelman, C.D.; Lu, Q.; Fardo, D.W.; Trittschuh, E.H.; Mez, J.; et al. Genetic Variants and Functional Pathways Associated with Resilience to Alzheimer's Disease. *Brain* **2020**, *143*, 2561–2575. [CrossRef] [PubMed]

96. Sędzikowska, A.; Szablewski, L. Insulin and Insulin Resistance in Alzheimer's Disease. *Int. J. Mol. Sci.* **2021**, *22*, 9987. [CrossRef] [PubMed]

97. Berlanga-Acosta, J.; Guillén-Nieto, G.; Rodríguez-Rodríguez, N.; Bringas-Vega, M.L.; García-Del-Barco-Herrera, D.; Berlanga-Saez, J.O.; García-Ojalvo, A.; Valdés-Sosa, M.J.; Valdés-Sosa, P.A. Insulin Resistance at the Crossroad of Alzheimer Disease Pathology: A Review. *Front. Endocrinol.* **2020**, *11*, 560375. [CrossRef]

98. Chen, Y.-C.; Chang, S.-C.; Lee, Y.-S.; Ho, W.-M.; Huang, Y.-H.; Wu, Y.-Y.; Chu, Y.-C.; Wu, K.-H.; Wei, L.-S.; Wang, H.-L.; et al. TOMM40 Genetic Variants Cause Neuroinflammation in Alzheimer's Disease. *Int. J. Mol. Sci.* **2023**, *24*, 4085. [CrossRef]

99. Kellar, D.; Craft, S. Brain Insulin Resistance in Alzheimer's Disease and Related Disorders: Mechanisms and Therapeutic Approaches. *Lancet Neurol.* **2020**, *19*, 758–766. [CrossRef]

100. Zheng, Z.; Li, Y.; Fan, S.; An, J.; Luo, X.; Liang, M.; Zhu, F.; Huang, K. WW Domain-Binding Protein 2 Overexpression Prevents Diet-Induced Liver Steatosis and Insulin Resistance through AMPKβ1. *Cell Death Dis.* **2021**, *12*, 228. [CrossRef]

101. Liu, Y.; He, E.; Zhang, Y.; Liu, Y.; Wang, Y.; Chen, S.; Wu, X.; Zeng, Y.; Leng, P. WW Domain Binding Protein 2 (WBP2) as an Oncogene in Breast Cancer: Mechanisms and Therapeutic Prospects—A Narrative Review. *Gland Surg.* **2022**, *11*, 1984–2002. [CrossRef]

102. Kim, D.H.; Perdomo, G.; Zhang, T.; Slusher, S.; Lee, S.; Phillips, B.E.; Fan, Y.; Giannoukakis, N.; Gramignoli, R.; Strom, S.; et al. FoxO6 Integrates Insulin Signaling With Gluconeogenesis in the Liver. *Diabetes* **2011**, *60*, 2763–2774. [CrossRef]

103. Lee, S.; Dong, H.H. FoxO Integration of Insulin Signaling with Glucose and Lipid Metabolism. *J. Endocrinol.* **2017**, *233*, R67–R79. [CrossRef] [PubMed]

104. PubChem INS—Insulin (Human). Available online: https://pubchem.ncbi.nlm.nih.gov/gene/INS/human (accessed on 19 February 2025).

105. Fridman, A.L.; Tainsky, M.A. Critical Pathways in Cellular Senescence and Immortalization Revealed by Gene Expression Profiling. *Oncogene* **2008**, *27*, 5975–5987. [CrossRef]

106. Wainberg, M.; Sinnott-Armstrong, N.; Mancuso, N.; Barbeira, A.N.; Knowles, D.A.; Golan, D.; Ermel, R.; Ruusalepp, A.; Quertermous, T.; Hao, K.; et al. Opportunities and Challenges for Transcriptome-Wide Association Studies. *Nat. Genet.* **2019**, *51*, 592–599. [CrossRef] [PubMed]

107. Wu, C.; Pan, W. A Powerful Fine-Mapping Method for Transcriptome-Wide Association Studies. *Hum. Genet.* **2020**, *139*, 199–213. [CrossRef] [PubMed]

108. Hunt, J.F.V.; Vogt, N.M.; Jonaitis, E.M.; Buckingham, W.R.; Koscik, R.L.; Zuelsdorff, M.; Clark, L.R.; Gleason, C.E.; Yu, M.; Okonkwo, O.; et al. Association of Neighborhood Context, Cognitive Decline, and Cortical Change in an Unimpaired Cohort. *Neurology* **2021**, *96*, e2500–e2512. [CrossRef]

109. Pohl, D.J.; Seblova, D.; Avila, J.F.; Dorsman, K.A.; Kulick, E.R.; Casey, J.A.; Manly, J. Relationship between Residential Segregation, Later-Life Cognition, and Incident Dementia across Race/Ethnicity. *Int. J. Environ. Res. Public Health* **2021**, *18*, 11233. [CrossRef]

110. Jang, J.B.; Hicken, M.T.; Mullins, M.; Esposito, M.; Sol, K.; Manly, J.J.; Judd, S.; Wadley, V.; Clarke, P.J. Racial Segregation and Cognitive Function Among Older Adults in the United States: Findings From the Reasons for Geographic and Racial Differences in Stroke Study. *J. Gerontol. B Psychol. Sci. Soc. Sci.* **2022**, *77*, 1132–1143. [CrossRef]

111. Forrester, S.N.; Gallo, J.J.; Whitfield, K.E.; Thorpe, R.J. A Framework of Minority Stress: From Physiological Manifestations to Cognitive Outcomes. *Gerontologist* **2019**, *59*, 1017–1023. [CrossRef]

112. Schulz, A.; Northridge, M.E. Social Determinants of Health: Implications for Environmental Health Promotion. *Health Educ. Behav.* **2004**, *31*, 455–471. [CrossRef]

113. Auchincloss, A.H.; Moore, K.A.; Moore, L.V.; Roux, A.V.D. Improving Retrospective Characterization of the Food Environment for a Large Region in the United States during a Historic Time Period. *Health Place* **2012**, *18*, 1341–1347. [CrossRef]

114. Powell, L.M.; Chaloupka, F.J.; Slater, S.J.; Johnston, L.D.; O'Malley, P.M. The Availability of Local-Area Commercial Physical Activity-Related Facilities and Physical Activity among Adolescents. *Am. J. Prev. Med.* **2007**, *33*, S292–S300. [CrossRef] [PubMed]

115. Gordon-Larsen, P.; Nelson, M.C.; Page, P.; Popkin, B.M. Inequality in the Built Environment Underlies Key Health Disparities in Physical Activity and Obesity. *Pediatrics* **2006**, *117*, 417–424. [CrossRef] [PubMed]

116. Finlay, J.; Esposito, M.; Li, M.; Kobayashi, L.C.; Khan, A.M.; Gomez-Lopez, I.; Melendez, R.; Colabianchi, N.; Judd, S.; Clarke, P.J. Can Neighborhood Social Infrastructure Modify Cognitive Function? A Mixed-Methods Study of Urban-Dwelling Aging Americans. *J. Aging Health* **2021**, *33*, 772–785. [CrossRef] [PubMed]

117. Besser, L.M.; McDonald, N.C.; Song, Y.; Kukull, W.A.; Rodriguez, D.A. Neighborhood Environment and Cognition in Older Adults: A Systematic Review. *Am. J. Prev. Med.* **2017**, *53*, 241–251. [CrossRef]

118. Rosso, A.L.; Flatt, J.D.; Carlson, M.C.; Lovasi, G.S.; Rosano, C.; Brown, A.F.; Matthews, K.A.; Gianaros, P.J. Neighborhood Socioeconomic Status and Cognitive Function in Late Life. *Am. J. Epidemiol.* **2016**, *183*, 1088–1097. [CrossRef]

119. Lang, I.A.; Llewellyn, D.J.; Langa, K.M.; Wallace, R.B.; Huppert, F.A.; Melzer, D. Neighborhood Deprivation, Individual Socioeconomic Status, and Cognitive Function in Older People: Analyses from the English Longitudinal Study of Ageing. *J. Am. Geriatr. Soc.* **2008**, *56*, 191–198. [CrossRef]

120. Shih, R.A.; Ghosh-Dastidar, B.; Margolis, K.L.; Slaughter, M.E.; Jewell, A.; Bird, C.E.; Eibner, C.; Denburg, N.L.; Ockene, J.; Messina, C.R. Neighborhood Socioeconomic Status and Cognitive Function in Women. *Am. J. Public Health* **2011**, *101*, 1721–1728. [CrossRef]

121. Wu, Y.-T.; Prina, A.M.; Jones, A.; Matthews, F.E.; Brayne, C. The Built Environment and Cognitive Disorders: Results From the Cognitive Function and Ageing Study II. *Am. J. Prev. Med.* **2017**, *53*, 25–32. [CrossRef]

122. Li, Q.S.; Sun, Y.; Wang, T. Epigenome-Wide Association Study of Alzheimer's Disease Replicates 22 Differentially Methylated Positions and 30 Differentially Methylated Regions. *Clin. Epigenet.* **2020**, *12*, 149. [CrossRef]

123. Yu, L.; Chibnik, L.B.; Srivastava, G.P.; Pochet, N.; Yang, J.; Xu, J.; Kozubek, J.; Obholzer, N.; Leurgans, S.E.; Schneider, J.A.; et al. Association of Brain DNA Methylation in SORL1, ABCA7, HLA-DRB5, SLC24A4, and BIN1 With Pathological Diagnosis of Alzheimer Disease. *JAMA Neurol.* **2015**, *72*, 15–24. [CrossRef]

124. De Jager, P.L.; Srivastava, G.; Lunnon, K.; Burgess, J.; Schalkwyk, L.C.; Yu, L.; Eaton, M.L.; Keenan, B.T.; Ernst, J.; McCabe, C.; et al. Alzheimer's Disease: Early Alterations in Brain DNA Methylation at ANK1, BIN1, RHBDF2 and Other Loci. *Nat. Neurosci.* **2014**, *17*, 1156–1163. [CrossRef] [PubMed]

125. Lunnon, K.; Smith, R.; Hannon, E.; De Jager, P.L.; Srivastava, G.; Volta, M.; Troakes, C.; Al-Sarraj, S.; Burrage, J.; Macdonald, R.; et al. Methylomic Profiling Implicates Cortical Deregulation of ANK1 in Alzheimer's Disease. *Nat. Neurosci.* **2014**, *17*, 1164–1170. [CrossRef] [PubMed]

126. Yamazaki, K.; Yoshino, Y.; Mori, T.; Yoshida, T.; Ozaki, Y.; Sao, T.; Mori, Y.; Ochi, S.; Iga, J.; Ueno, S. Gene Expression and Methylation Analysis of ABCA7 in Patients with Alzheimer's Disease. *J. Alzheimer's Dis.* **2017**, *57*, 171–181. [CrossRef] [PubMed]

127. Diez Roux, A.V.; Mair, C. Neighborhoods and Health. *Ann. N. Y. Acad. Sci.* **2010**, *1186*, 125–145. [CrossRef]

128. Yen, I.H.; Michael, Y.L.; Perdue, L. Neighborhood Environment in Studies of Health of Older Adults: A Systematic Review. *Am. J. Prev. Med.* **2009**, *37*, 455–463. [CrossRef]

129. Lisabeth, L.; Diez Roux, A.; Escobar, J.; Smith, M.; Morgenstern, L. Neighborhood Environment and Risk of Ischemic Stroke: The Brain Attack Surveillance in Corpus Christi (BASIC) Project. *Am. J. Epidemiol.* **2007**, *165*, 279–287. [CrossRef]

130. Brown, A.F.; Liang, L.-J.; Vassar, S.D.; Stein-Merkin, S.; Longstreth, W.T., Jr.; Ovbiagele, B.; Yan, T.; Escarce, J.J. Neighborhood Disadvantage and Ischemic Stroke: The Cardiovascular Health Study (CHS). *Stroke* **2011**, *42*, 3363–3368. [CrossRef]

131. Chaar, D.L.; Tu, L.; Moore, K.; Du, J.; Opsasnick, L.A.; Ratliff, S.M.; Mosley, T.H.; Kardia, S.L.R.; Zhao, W.; Zhou, X.; et al. Neighborhood Environment Associations with Cognitive Function and Structural Brain Measures in Older African Americans. *BMC Med.* **2025**, *23*, 15. [CrossRef]

132. Chaar, D.L.; Nguyen, K.; Wang, Y.-Z.; Ratliff, S.M.; Mosley, T.H.; Kardia, S.L.R.; Smith, J.A.; Zhao, W. SNP-by-CpG Site Interactions in ABCA7 Are Associated with Cognition in Older African Americans. *Genes* **2022**, *13*, 2150. [CrossRef]

133. Besser, L.; Galvin, J.E.; Rodriguez, D.; Seeman, T.; Kukull, W.; Rapp, S.R.; Smith, J. Associations between Neighborhood Built Environment and Cognition Vary by Apolipoprotein E Genotype: Multi-Ethnic Study of Atherosclerosis. *Health Place* **2019**, *60*, 102188. [CrossRef]

134. Smith, J.A.; Kho, M.; Zhao, W.; Yu, M.; Mitchell, C.; Faul, J.D. Genetic Effects and Gene-by-Education Interactions on Episodic Memory Performance and Decline in an Aging Population. *Soc. Sci. Med.* **2021**, *271*, 112039. [CrossRef]

135. Husain, M.A.; Laurent, B.; Plourde, M. APOE and Alzheimer's Disease: From Lipid Transport to Physiopathology and Therapeutics. *Front. Neurosci.* **2021**, *15*, 630502. [CrossRef] [PubMed]

136. Yamazaki, Y.; Zhao, N.; Caulfield, T.R.; Liu, C.-C.; Bu, G. Apolipoprotein E and Alzheimer Disease: Pathobiology and Targeting Strategies. *Nat. Rev. Neurol.* **2019**, *15*, 501–518. [CrossRef] [PubMed]

137. McQuade, A.; Kang, Y.J.; Hasselmann, J.; Jairaman, A.; Sotelo, A.; Coburn, M.; Shabestari, S.K.; Chadarevian, J.P.; Fote, G.; Tu, C.H.; et al. Gene Expression and Functional Deficits Underlie TREM2-Knockout Microglia Responses in Human Models of Alzheimer's Disease. *Nat. Commun.* **2020**, *11*, 5370. [CrossRef] [PubMed]

138. Mirescu, C.; Dejanovic, B.; Larson, K.C.; Kiragasi, B.; Gergits, F.W.; Figley, M.D.; Renoux, A.J.; Huang, L.; Pandya, B.A.; Houze, J.B.; et al. Pharmacological and Functional Characterization of the First Small Molecule TREM2 Agonist, VG-3927, for the Treatment of Alzheimer's Disease. *Alzheimer's Dement.* **2025**, *20*, e089318. [CrossRef]

139. Bourquard, T.; Lee, K.; Al-Ramahi, I.; Pham, M.; Shapiro, D.; Lagisetty, Y.; Soleimani, S.; Mota, S.; Wilhelm, K.; Samieinasab, M.; et al. Functional Variants Identify Sex-Specific Genes and Pathways in Alzheimer's Disease. *Nat. Commun.* **2023**, *14*, 2765. [CrossRef]

140. Andrews, S.J.; Renton, A.E.; Fulton-Howard, B.; Podlesny-Drabiniok, A.; Marcora, E.; Goate, A.M. The Complex Genetic Architecture of Alzheimer's Disease: Novel Insights and Future Directions. *eBioMedicine* **2023**, *90*, 104511. [CrossRef]

141. Yang, X.; Wen, J.; Yang, H.; Jones, I.R.; Zhu, X.; Liu, W.; Li, B.; Clelland, C.D.; Luo, W.; Wong, M.Y.; et al. Functional Characterization of Alzheimer's Disease Genetic Variants in Microglia. *Nat. Genet.* **2023**, *55*, 1735–1744. [CrossRef]

142. Cheng, L.; Chen, C.; Guo, W.; Liu, K.; Zhao, Q.; Lu, P.; Yu, F.; Xu, X. EFEMP1 Overexpression Contributes to Neovascularization in Age-Related Macular Degeneration. *Front. Pharmacol.* **2021**, *11*, 547436. [CrossRef]

143. Li, B.; Ritchie, M.D. From GWAS to Gene: Transcriptome-Wide Association Studies and Other Methods to Functionally Understand GWAS Discoveries. *Front. Genet.* **2021**, *12*, 713230. [CrossRef]

144. Gusev, A.; Ko, A.; Shi, H.; Bhatia, G.; Chung, W.; Penninx, B.W.J.H.; Jansen, R.; de Geus, E.J.C.; Boomsma, D.I.; Wright, F.A.; et al. Integrative Approaches for Large-Scale Transcriptome-Wide Association Studies. *Nat. Genet.* **2016**, *48*, 245–252. [CrossRef] [PubMed]

145. Zhu, H.; Zhou, X. Transcriptome-Wide Association Studies: A View from Mendelian Randomization. *Quant. Biol.* **2021**, *9*, 107–121. [CrossRef] [PubMed]

146. Liu, L.; Zeng, P.; Xue, F.; Yuan, Z.; Zhou, X. Multi-Trait Transcriptome-Wide Association Studies with Probabilistic Mendelian Randomization. *Am. J. Hum. Genet.* **2021**, *108*, 240–256. [CrossRef] [PubMed]

147. Yuan, Z.; Zhu, H.; Zeng, P.; Yang, S.; Sun, S.; Yang, C.; Liu, J.; Zhou, X. Testing and Controlling for Horizontal Pleiotropy with Probabilistic Mendelian Randomization in Transcriptome-Wide Association Studies. *Nat. Commun.* **2020**, *11*, 3861. [CrossRef]

148. Daniels, P.R.; Kardia, S.L.R.; Hanis, C.L.; Brown, C.A.; Hutchinson, R.; Boerwinkle, E.; Turner, S.T.; Genetic Epidemiology Network of Arteriopathy study. Familial Aggregation of Hypertension Treatment and Control in the Genetic Epidemiology Network of Arteriopathy (GENOA) Study. *Am. J. Med.* **2004**, *116*, 676–681. [CrossRef]

149. Delaneau, O.; Zagury, J.-F.; Marchini, J. Improved Whole-Chromosome Phasing for Disease and Population Genetic Studies. *Nat. Methods* **2013**, *10*, 5–6. [CrossRef]

150. Howie, B.N.; Donnelly, P.; Marchini, J. A Flexible and Accurate Genotype Imputation Method for the Next Generation of Genome-Wide Association Studies. *PLoS Genet.* **2009**, *5*, e1000529. [CrossRef]

151. Gogarten, S.M.; Sofer, T.; Chen, H.; Yu, C.; Brody, J.A.; Thornton, T.A.; Rice, K.M.; Conomos, M.P. Genetic Association Testing Using the GENESIS R/Bioconductor Package. *Bioinformatics* **2019**, *35*, 5346–5348. [CrossRef]

152. R: The R Project for Statistical Computing. Available online: https://www.r-project.org/ (accessed on 14 June 2022).

153. Lockstone, H.E. Exon Array Data Analysis Using Affymetrix Power Tools and R Statistical Software. *Brief. Bioinform.* **2011**, *12*, 634–644. [CrossRef]

154. Irizarry, R.A.; Bolstad, B.M.; Collin, F.; Cope, L.M.; Hobbs, B.; Speed, T.P. Summaries of Affymetrix GeneChip Probe Level Data. *Nucleic Acids Res.* **2003**, *31*, e15. [CrossRef]

155. Dai, M.; Wang, P.; Boyd, A.D.; Kostov, G.; Athey, B.; Jones, E.G.; Bunney, W.E.; Myers, R.M.; Speed, T.P.; Akil, H.; et al. Evolving Gene/Transcript Definitions Significantly Alter the Interpretation of GeneChip Data. *Nucleic Acids Res.* **2005**, *33*, e175. [CrossRef] [PubMed]

156. Saha, A.; Battle, A. False Positives in Trans-eQTL and Co-Expression Analyses Arising from RNA-Sequencing Alignment Errors. *F1000Research* **2018**, *7*, 1860. [CrossRef]

157. Johnson, W.E.; Li, C.; Rabinovic, A. Adjusting Batch Effects in Microarray Expression Data Using Empirical Bayes Methods. *Biostatistics* **2007**, *8*, 118–127. [CrossRef] [PubMed]

158. Barbeira, A.N.; Bonazzola, R.; Gamazon, E.R.; Liang, Y.; Park, Y.; Kim-Hellmuth, S.; Wang, G.; Jiang, Z.; Zhou, D.; Hormozdiari, F.; et al. Exploiting the GTEx Resources to Decipher the Mechanisms at GWAS Loci. *Genome Biol.* **2021**, *22*, 49. [CrossRef] [PubMed]

159. The GTEx Consortium. The GTEx Consortium Atlas of Genetic Regulatory Effects across Human Tissues. *Science* **2020**, *369*, 1318–1330. [CrossRef]

160. Turner, S.D. Qqman: An R Package for Visualizing GWAS Results Using Q-Q and Manhattan Plots 2014, 005165. Available online: https://www.biorxiv.org/content/10.1101/005165.abstract (accessed on 1 August 2023).

161. Berisa, T.; Pickrell, J.K. Approximately Independent Linkage Disequilibrium Blocks in Human Populations. *Bioinformatics* **2016**, *32*, 283. [CrossRef]

162. Chen, H.; Boutros, P.C. VennDiagram: A Package for the Generation of Highly-Customizable Venn and Euler Diagrams in R. *BMC Bioinform.* **2011**, *12*, 35. [CrossRef]

163. de Leeuw, C.A.; Stringer, S.; Dekkers, I.A.; Heskes, T.; Posthuma, D. Conditional and Interaction Gene-Set Analysis Reveals Novel Functional Pathways for Blood Pressure. *Nat. Commun.* **2018**, *9*, 3768. [CrossRef]

164. Mancarcı, B.O. Gene Synonym 2022. Available online: https://github.com/oganm/geneSynonym (accessed on 1 August 2023).

165. Raudvere, U.; Kolberg, L.; Kuzmin, I.; Arak, T.; Adler, P.; Peterson, H.; Vilo, J. G:Profiler: A Web Server for Functional Enrichment Analysis and Conversions of Gene Lists (2019 Update). *Nucleic Acids Res.* **2019**, *47*, W191–W198. [CrossRef]